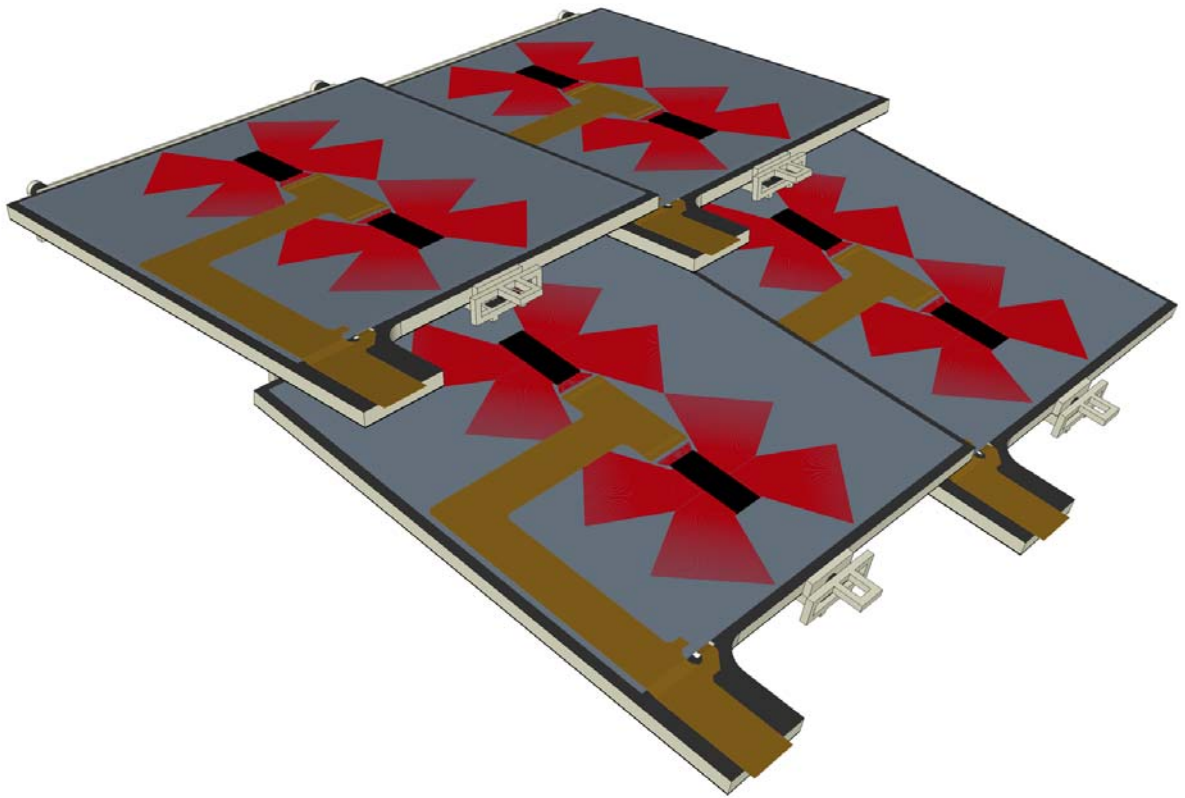




**SiD Tracker
R&D
Report**



**SiD Tracker R&D Report
Submitted to the World-Wide Study Detector R&D Panel
Tuesday, January 30, 2007**

(This page intentionally left blank)

CONTENTS

| | |
|--------------------------------------|----|
| 1 Introduction..... | 6 |
| 2 Outer Tracker Design..... | 8 |
| 2.1 Introduction..... | 8 |
| 3 Tracker modules..... | 12 |
| 3.1 Introduction..... | 12 |
| 3.2 Module Design..... | 12 |
| 3.3 Sensor Design | 14 |
| 3.4 Status and R&D Needs | 16 |
| 3.5 Thin Silicon..... | 18 |
| 4 Sensor testing..... | 23 |
| 4.1 General Requirements..... | 23 |
| 5 Front-end Readout | 26 |
| 5.1 Introduction..... | 26 |
| 5.2 KPiX Readout Chip | 26 |
| 5.2.1 Signal-to-noise Ratio | 27 |
| 5.2.2 Status and R&D Needs | 28 |
| 5.3 Power Distribution and DAQ..... | 29 |
| 5.3.1 Status and R&D Needs | 30 |
| 5.4 Time-over-Threshold Readout..... | 31 |
| 5.4.1 Introduction..... | 31 |
| 5.4.2 R&D Needed..... | 32 |
| 5.5 Charge Division Readout..... | 32 |
| 5.5.1 Introduction..... | 32 |
| 5.5.2 Simulation Studies | 36 |

| | |
|--|----|
| 5.5.3 Test Sensors | 36 |
| 5.5.4 Readout Electronics | 36 |
| 5.5.5 Performance Characterization..... | 36 |
| 6 Readout cable..... | 37 |
| 6.1 Introduction..... | 37 |
| 6.1.1 Status and R&D Needs | 38 |
| 7 Mechanical Design, Structures, And Infrastructure..... | 39 |
| 7.1 Overview..... | 39 |
| 7.2 Status and R&D Needs | 39 |
| 7.3 Tracker Alignment..... | 42 |
| 8 Tracker Real-Time Alignment System | 45 |
| 8.1 Overview..... | 45 |
| 8.2 Status and R&D Needs | 45 |
| 9 Tracking simulation and performance | 49 |
| 9.1 Introduction..... | 49 |
| 9.2 Tracking Simulation Infrastructure..... | 49 |
| 9.3 Tracking Algorithms..... | 50 |
| 9.3.1 Vertex Detector Based Track Seeding..... | 51 |
| 9.3.2 Vertex Seeded Outer Tracking..... | 52 |
| 9.3.3 Stand Alone Tracking in the Outer Tracker..... | 52 |
| 9.3.4 Calorimeter Assisted Tracking | 53 |
| 9.4 Tracking Pattern Recognition Performance..... | 54 |
| 9.5 Tracking Resolution Studies | 58 |
| 9.6 R&D Plans for Tracking Simulation and Performance Studies..... | 60 |
| 10 Summary of r&d needs | 61 |

11 Summary..... 64

1 INTRODUCTION

Within the SiD detector concept the tracking system is to be regarded as an integrated tracking system. Individual detector components can be identified in the vertexing and tracking system, but the overall design is driven by the combined performance of the pixel detector at small radius, the outer strip detector at large radius and the electromagnetic calorimeter for the identification of minimum ionizing track stubs. The physics at the ILC requires efficient track reconstruction and excellent momentum resolution over nearly the full solid angle, even for tightly collimated jets. The main element for the pattern recognition is the highly pixellated vertex detector. The first step in track finding relies on identifying tracks in the vertex detector, where pattern recognition is simplified by the fact that precise three-dimensional information is available for each hit. Tracks found in the vertex detector are then propagated into the outer tracker, picking up additional hits and measuring the track curvature. However, an important class of events, notably strange particle decays and a few highly boosted b-quarks, will decay at radii that do not allow for pattern recognition in the vertex detector because there are either too few hits, or simply because the decay occurs outside the vertex detector. If these particles decay before reaching the outer tracker, their tracks can be reconstructed by a stand-alone tracking algorithm using the outer tracker. In a third class of events, tracks produced by decays inside the outer tracker can be reconstructed by a calorimeter-assisted tracking algorithm. Obvious examples are long-lived particles such as K_S^0 and Lambdas, as well as new physics signatures that would include long-lived exotic particles like those predicted by some gauge-mediated supersymmetry breaking scenarios. Reconstructing kinked tracks produced by particles that lose a substantial portion of their energy in the tracker, as well as reconstructing backscatters from the calorimeter are other possibilities. The calorimeter-assisted algorithm uses the electromagnetic calorimeter to provide seeds for pattern recognition in the tracker. The very fine segmentation of the EM calorimeter allows for detection of traces left by minimum ionizing particles and uses them to determine the track entry point, direction, and sometimes curvature with a precision sufficient for extrapolating the track back into the tracker. This set of complementary algorithms provides for very robust pattern recognition and track finding.

One of the characteristics of an e^+e^- collider is that most processes occur through an s-channel spin-1 boson exchange, resulting in an angular distribution that puts a premium on the forward region. Furthermore, many physics processes with polarized beams show great sensitivity to deviations from the standard model in the forward regions. It is fair to say that in many existing collider experiments the forward tracking detectors were far from optimal. Given the low event rates at the ILC, as well as the checkered history of the physics community in designing and building vertex detectors and trackers optimized for the forward regions, significant R&D is needed not just in the mechanical design but also in the simulation area to ensure high tracking efficiency and excellent heavy flavor identification in the forward region.

The SiD Central Tracker is based on silicon microstrip sensors, arranged in 5 barrel and 4 endcap layers. These devices offer several advantages for ILC tracking. Microstrip sensors have inherently high precision, which, along with the 5T SiD solenoidal field, translates into superb tracker momentum resolution. Microstrip sensors have excellent two-track resolution, ensuring fully efficient tracking in the core of dense jets. With proper attention to detail, the thickness of the individual tracker layers can be reduced to $\sim 0.8\% X_0$. So, this tracker design, in contrast to

some others, presents little material before the electromagnetic calorimetry in the forward direction. Lepton ID and Particle Flow Calorimetry will benefit accordingly. Silicon sensors are fast, so the SiD tracker will be sensitive only to the bunch crossing of physics interest, and free of the backgrounds which integrate during the entire bunch train. Finally, the SiD tracker will be robust against errant machine backgrounds, not be damaged, and not trip when showering particles or unexpected synchrotron radiation hit the detector.

Serious R&D for the SiD Tracker began more than three years ago, and has encompassed physics studies to understand the importance of excellent momentum resolution, characterizations of the tracker performance, the development of pattern recognition and track fitting codes, full Geant4 tracker descriptions, mechanical designs for the supporting structures and sensor modules, laser alignment systems, and most recently sensor designs. Work has also been ongoing on two different readout chip possibilities. In 2007, we hope to build and test new sensors, develop and test microstrip readouts and cables suitable for the SiD tracker, and begin mechanical prototyping. Detailed system design and optimization, especially for the forward tracker, will also proceed, and we'll work toward a selection of technologies for the tracker.

In the following, we discuss the SiD Silicon Outer Tracker in some detail. The outer tracker design is discussed in section 2, the silicon sensors and sensor modules in section 3, plans for sensor testing in section 4, the front end readout in section 5, the readout cable in section 6, the mechanical design in section 7, and the alignment system in section 8. The performance of the tracking system and the needed software development is reviewed in section 9. Section 10 tabulates the manpower and funding request of all the groups involved in the SiD tracker. A brief summary in section 11 concludes the report.

2 OUTER TRACKER DESIGN

2.1 Introduction

The all-silicon outer tracker combines barrel and disk geometries and includes associated readout, cabling, support, cooling, and monitoring systems. Its design is based upon a preliminary optimization of the physics performance of the entire detector, while at the same time satisfying various boundary conditions. The requirement that the vertex detector be accessible for servicing limits the inner radius. The requirement that the tracker fits within the electromagnetic calorimeters limits its outer radius and length. The outer silicon tracker consists of five nested barrels in the central region and four disks in each of the end regions. The barrel supports are continuous cylinders formed from a sandwich of carbon fiber - resin composite around a Rohacell core. The disks are also double-walled carbon fiber structures around a Rohacell core. Each disk is supported from the end of a barrel. Spoked annular rings support the ends of each barrel cylinder from the inner surface of the next barrel outward. It is envisioned that the electronics and power cables that supply entire segments of the detector are mounted on those spoked rings. The dimensions of the barrels and disks are given in Table 1. Figure 1 shows an elevation view of the outer tracker.

| | Barrel Silicon | | End Cap Silicon | |
|-------------------|----------------|------------------|-----------------|--------------|
| | R (cm) | Half-length (cm) | Z (cm) | R (cm) |
| Barrel 1 | 22.0 | 55.8 | | |
| Barrel 2 / Disk 1 | 47.0 | 82.5 | 85.7 | 20.7 – 49.4 |
| Barrel 3 / Disk 2 | 72.0 | 108.3 | 111.6 | 20.7 – 74.7 |
| Barrel 4 / Disk 3 | 97.0 | 134.7 | 138.0 | 20.7 – 99.9 |
| Barrel 5 / Disk 4 | 122.0 | 160.6 | 163.8 | 20.7 – 125.0 |

Table 1 Outer tracker geometry

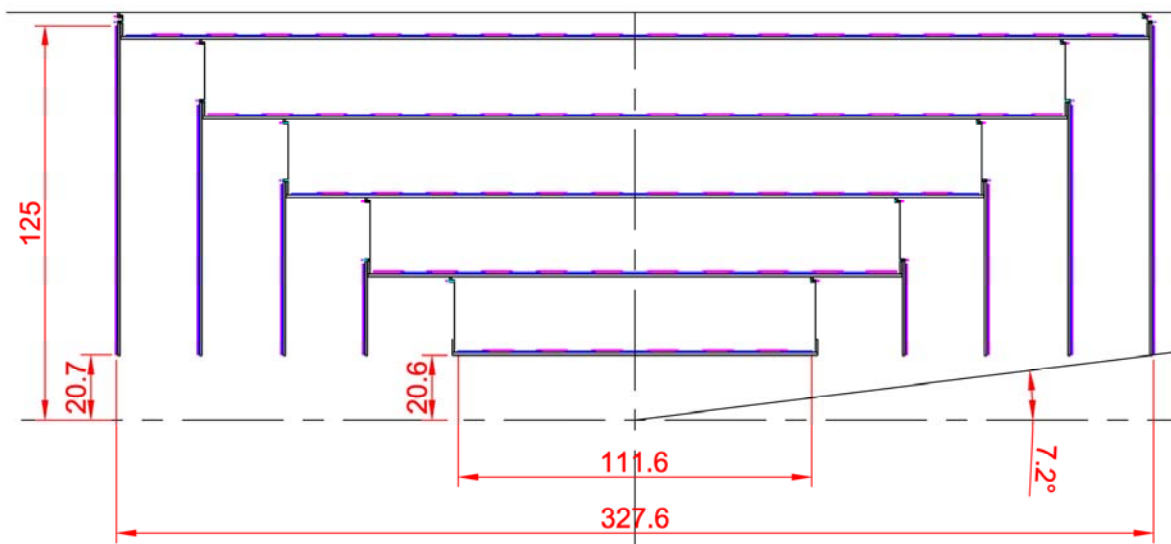


Figure 1: Elevation view of the outer tracker. Dimensions are in cm.

Because of the very low occupancies in the outer barrel, the nominal design for the outer tracker employs only axial readout in the barrel region. In the baseline design, the barrels are covered with silicon modules. Modules are comprised of a carbon fiber composite frame with Rohacell/epoxy cross bracing and have one single-sided silicon sensor bonded to the outer surface. Sensors are obtained from one single 6" wafer and are approximately 10cm by 10cm. This size sets the longitudinal readout segmentation of the barrel detectors. The sensors are 300 μm thick and have strip and readout pitches of 25 μm and 50 μm , respectively. Hermetic coverage is obtained by ensuring small overlaps between sensors, both longitudinally and azimuthally. Azimuthal overlap is obtained by slightly tilting the sensors. The angle by which the sensor is tilted compensates for the Lorentz angle of the collected charge in the 5T field of the solenoid. Longitudinal overlap is obtained by placing alternate sensors at slightly different radii. Figure 2 shows an R ϕ -view of the barrel region of the outer tracker. Modules are attached to the cylinder using a PEEK mounting clip. The readout chips and cables are mounted directly to the outer surface of the silicon sensors. The cables supply power and control to the readout chip from electronics located at the ends of the barrel.

For pattern recognition, the disks will provide 3d-space points. The current design has both sides of the disks covered with silicon modules. The modules on one side provide the R-readout and the modules on the other side provide the ϕ -readout. Also in the forward region sensors will be 300 μm thick with intermediate strips. Since the sensors will be wedge shaped, the pitch will vary with radius.

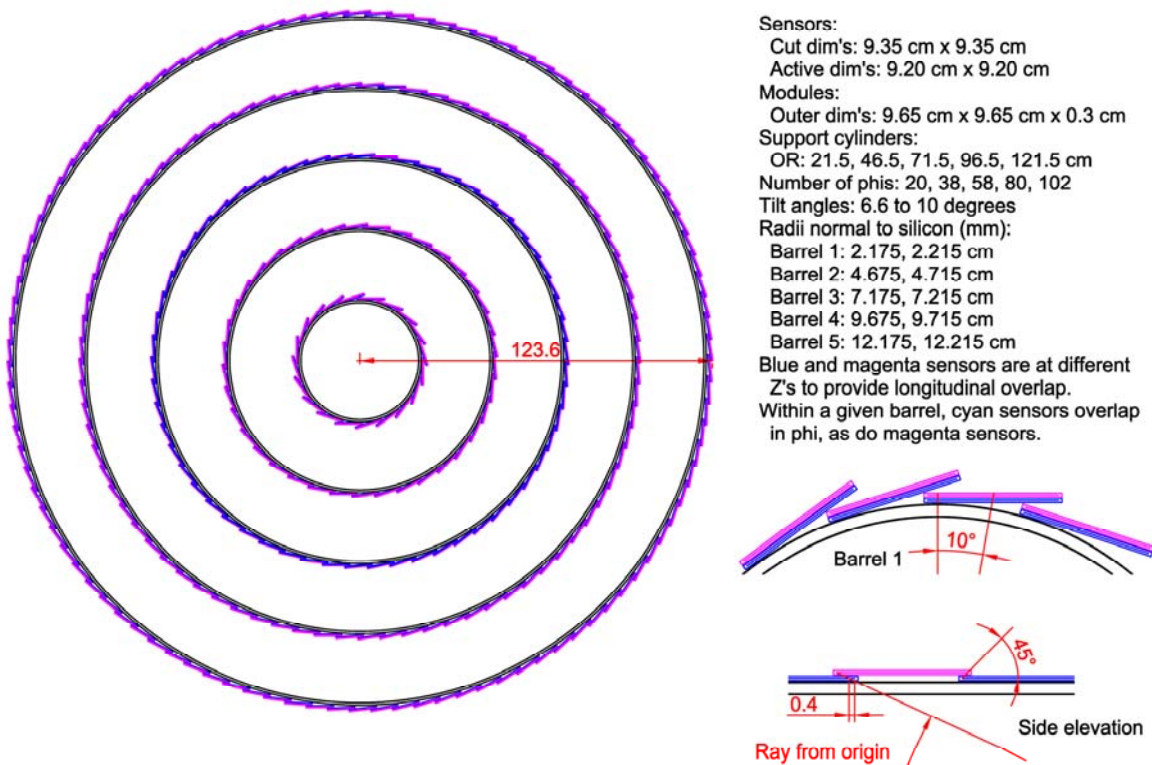


Figure 2: End view of the outer tracker. The inset shows overlaps in ϕ and z of the silicon modules

The outer tracker design allows the tracker itself and vertex detector elements to be serviced without disconnecting the beam pipe from elements of the beam delivery system. During servicing, temporary support will be provided to the outer tracker to allow it to be rolled longitudinally while vertex detector elements and the beam pipe remain fixed, as shown in Figure 3. That motion, the present dimensions of the beam delivery system, and the requirement that there be radial clearance set a minimum radius of approximately 20.5 cm for outer tracker structures. Three small-radius, forward disks per end extend tracker acceptance and pattern recognition capabilities to smaller cone angles. Because those disks share radial location, support, cooling, and possibly sensor technologies with the vertex detector, they will be considered elements of the vertex detector for purposes of this review.

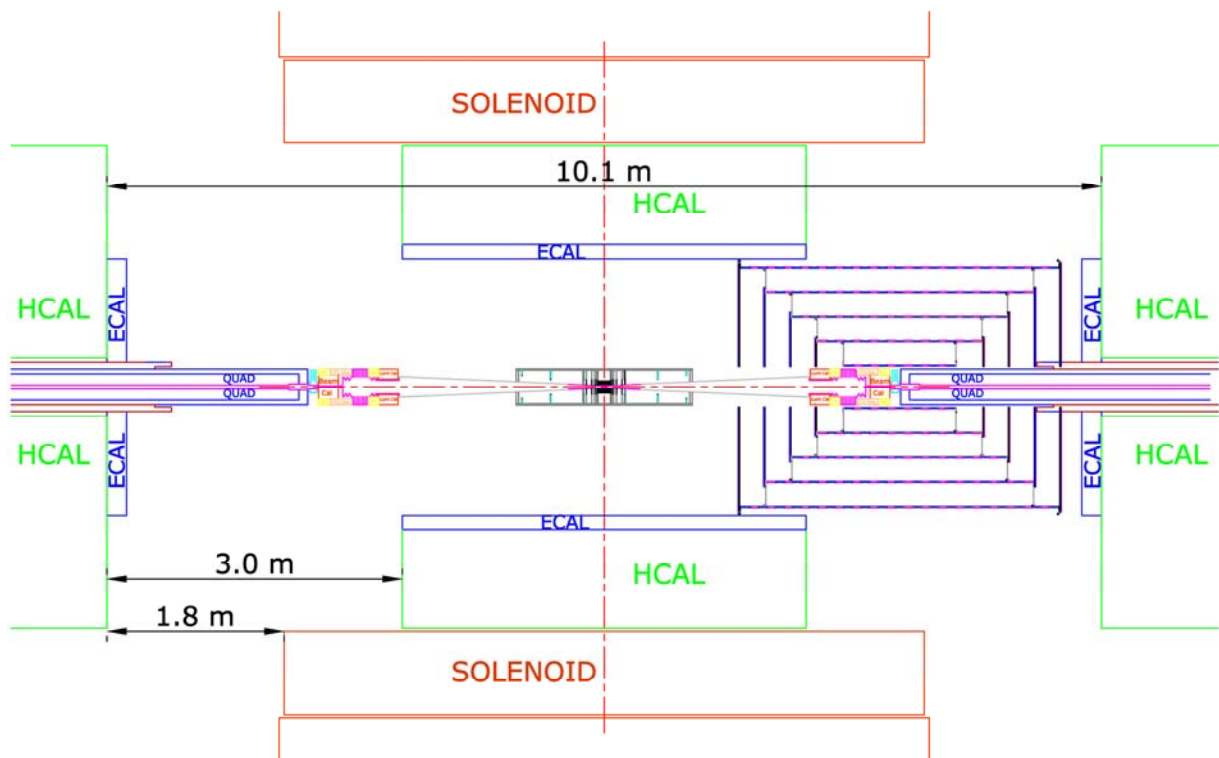


Figure 3: Configuration with the detector open for access to the vertex detector.

Figure 4 shows the cumulative amount of material as function of polar angle as modeled in the Monte Carlo. The lowest curve shows the contribution from the beam pipe and the readout for the vertex detector. The material corresponding to the various readout elements has conservatively been assumed to be uniformly distributed in the tracker volume. The following two curves indicate the additional material due to the active vertex detector elements and the supports, respectively. The outer curve gives the amount of material of the tracker as a whole, that is, the sum of the vertex detector and the outer tracker and anticipated dead material in the tracking volume. Overall a material budget of about $0.8\% X_0$ per layer is achieved for the outer tracker.

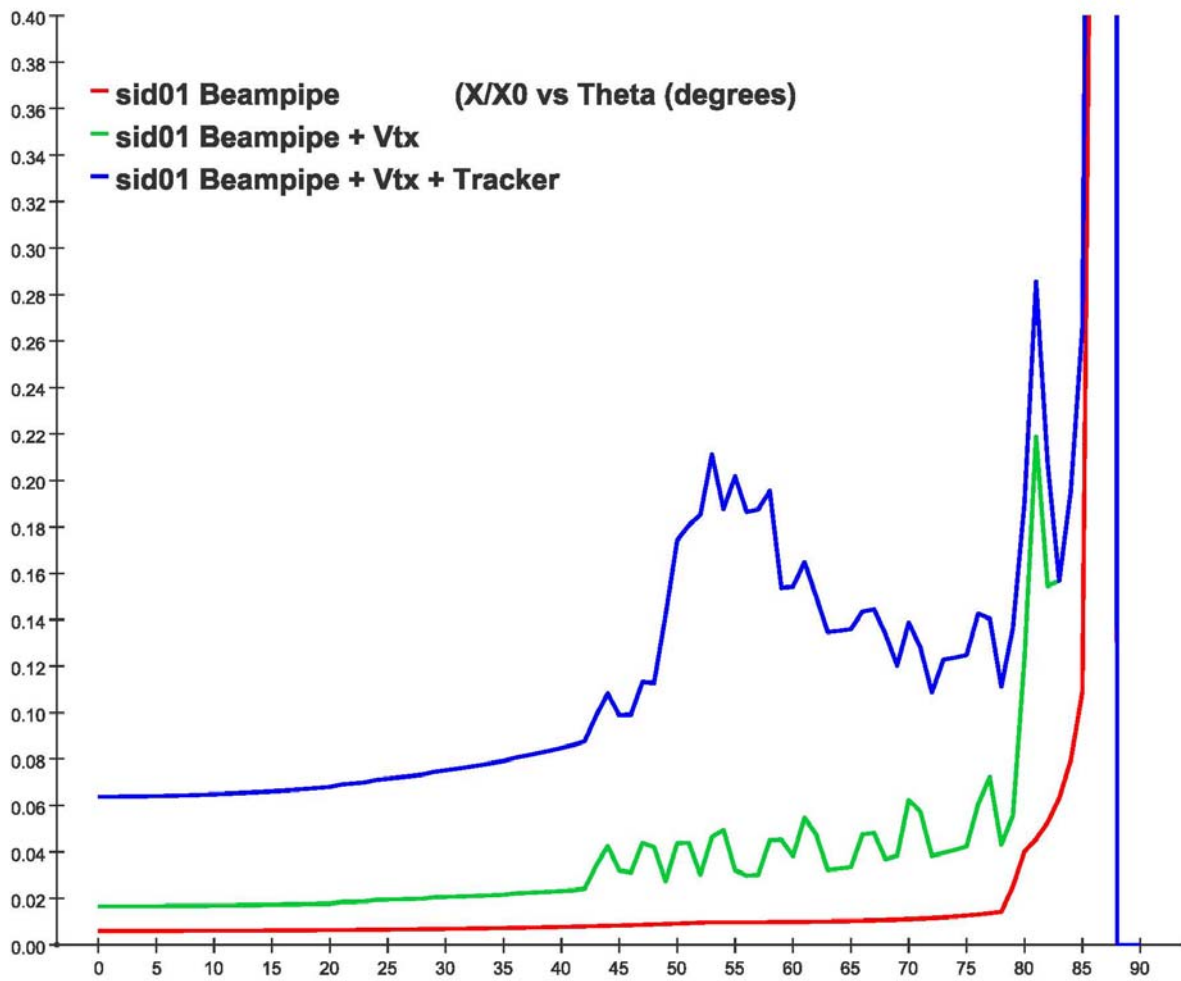


Figure 4: Total material budget of the tracker as fraction of a radiation length as function of 90° - polar angle as modeled in the Monte Carlo

3 TRACKER MODULES

3.1 Introduction

The ILC experiments demand tracking systems unlike any previously envisioned. In addition to efficient and robust track-finding, the momentum resolution required to enable precision physics at ILC energies must improve significantly upon that of previous trackers. The design must minimize material in front of the calorimeter that might endanger particle-flow jet reconstruction. Even with the largest feasible magnetic field, the tracking volume is quite large so that tracker components must be inexpensively and easily mass-produced. Finally, the tracker must be robust against beam-related accidents and aging.

Silicon microstrips are the clear choice to achieve the best tracking precision and durability, but a mass-produced silicon tracker has never before been assembled within an acceptable material budget. The design of the SiD tracker modules is key to meeting these requirements. Novel designs for sensors and readout chips exploit the ILC timing structure to eliminate the hybrid circuit board and liquid cooling, drastically reducing the mass penalty for having a large number of readout channels. This freedom allows the sensor design and tracker layout to be optimized for the best single-hit precision and pattern recognition: fine-pitch sensors with short strips to achieve high signal-to-noise and low occupancies.

While most elements of this approach utilize well-established technologies, their novel implementation in the SiD tracker requires significant R&D to overcome key obstacles. The success of the unorthodox readout scheme depends upon innovative readout chips and double-metal sensors and mastering RF pickup issues that often prove difficult. The mechanical design relies upon the industrial manufacture of high-performance composites and ceramics and unproven assembly techniques to achieve low mass and simplified production. As a result, only the assembly and operation of full working prototypes can establish the validity of this concept.

3.2 Module Design

The module is the most elementary working component of the SiD tracker and achieves low mass and simplicity through minimalist design. The single-sided barrel module has only a single, square sensor with a pair of KPiX readout chips and a short Kapton[®] readout “pigtail” mounted to the face of a carbon-fiber/Rohacell[®]/Torlon[®] support frame with silicon-nitride balls for precision mounting. The support frame attaches to an injection-molded Torlon[®] clip that glues to the support cylinders. There is no hybrid circuit board or mechanical cooling path since gas flow can provide the required cooling. The barrel module design is shown in Figure 5 and represents roughly 0.5% X_0 per unit coverage including longer readout cables needed to connect the pigtails to the power and readout distribution boards mounted on the support rings at the ends of the barrels. This module design can be made double-sided by placing the same silicon and readout on both sides, allowing either small-angle or 90-degree stereo modules and resulting in modules with roughly 0.9% X_0 per unit coverage. Although a detailed design for the forward modules awaits further simulation study, it is presumed that forward modules will be of similar double-sided design.

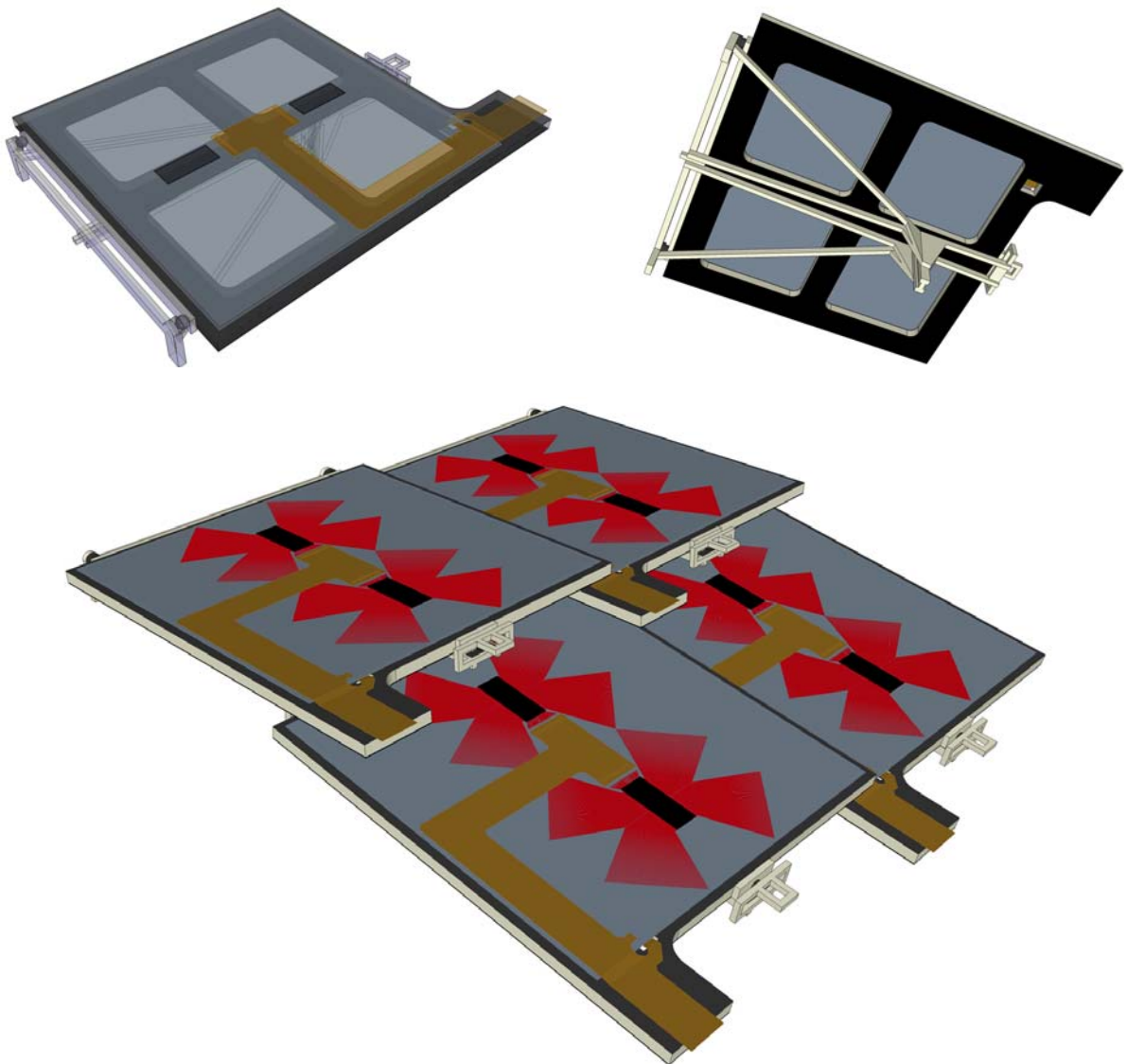


Figure 5: A barrel module attached to its mounting clip from above and below (top) and a set of four modules as mounted to a cylinder, illustrating overlaps in both ϕ and z (bottom).

The KPiX chips are bump-bonded directly to the face of the sensor, and the readout strips of the sensor connect to the bonding array via double-metal traces (see Figure 6). A necessary complication of this scheme is that the power, control and readout signals of KPiX must also be routed to a bonding array for the pigtail cable on the double-metal layer. The pigtail is simply glued to the face of the sensor and wirebonded to these traces. This novel readout configuration, responsible for both mass reduction and assembly simplification, creates some key R&D issues.

The other important issues result from the module support concept, which focuses on achieving industrial mass-producibility for all components and little or no on-site assembly. The support

frame is composed of a pair of thin, high-modulus carbon-fiber skins sandwiched around a Rohecell core. The frame has injection-molded carbon-filled Torlon strips on two edges into which the precision silicon-nitride balls that provide a kinematic, three-point mount are insert-molded. The mounting clips are manufactured in the same way and include custom silicon nitride mating parts for the mounting balls of the support frame. In principle, all of these components can be mass produced and have minimal per-unit costs in the quantities needed for the detector. However, proving that this design simultaneously meets our mass, precision and stability requirements requires significant R&D. Further investigation is also needed to firmly establish that this concept can be industrially mass produced at an attractive cost.

3.3 Sensor Design

The sensors for the SiD tracker are largely conventional and their design is based upon previous sensors with which we have considerable experience: single-sided, double-metal, p+/n sensors with 25 micron sense pitch and 50 micron readout. This floating-strip design provides the best possible single-hit resolution for a reasonable channel count as long as S/N remains large, as shown in Figure 9, motivating the use of short readout strips to reduce capacitance. The baseline assumes that these sensors are 300-microns thick, however, the use of thinned sensors will be possible without compromising single-hit resolution if KPiX meets design goals for noise performance. A reduced set of specifications for prototype barrel sensors are shown in Table 2 and a picture showing the double-metal layout is shown in Figure 6.

The novel use of double-metal for bump bonding and relaying readout and power creates several key issues that will require R&D to address. We must establish that bump-bonding silicon strip detectors presents no issues for processing, assembly or the performance of the channels that underlie the chip. We must also show that an optimized design for the double-metal layer delivers the required capacitance and series resistance for all channels to provide uniform pedestals and noise performance. Most importantly, it must be shown that any pickup or power supply issues that result from using traces on the double metal layer to transmit control and data signals and provide power to KPiX can be satisfactorily resolved. The presence of a synchronous LVDS clock and fluctuations in DVDD during the passage of the bunch train are the focal points of this investigation.

To date, R&D has concentrated on the barrel sensors, as the tracking requirements in the barrel are relatively well understood. Meanwhile, it has been assumed that the forward sensors will be essentially the same regardless of shape and strip orientation. However, some possible designs for the forward sensors might require additional R&D if they rely upon novel elements that are not simple extrapolations of their counterparts in the barrel.

| Parameter | Specification |
|----------------------------------|-----------------------|
| Wafer size | 6-inch |
| Active area | 92.031 mm X 92.031 mm |
| Number of readout (sense) strips | 1840 (3679) |
| Depletion voltage | <100V |
| Junction breakdown | >200V |
| Leakage current | < 4 μ A at 150V |
| Strip width | 7-8 μ m |
| Coupling capacitance | >10pF/cm |
| Interstrip capacitance | <1.2pF/cm |
| Polysilicon bias resistor value | 20 \pm 2 M Ω |
| Not working strips | <20 |

Table 2: The basic specifications for the prototype barrel silicon sensors. Specifications for forward sensors are expected to be similar.

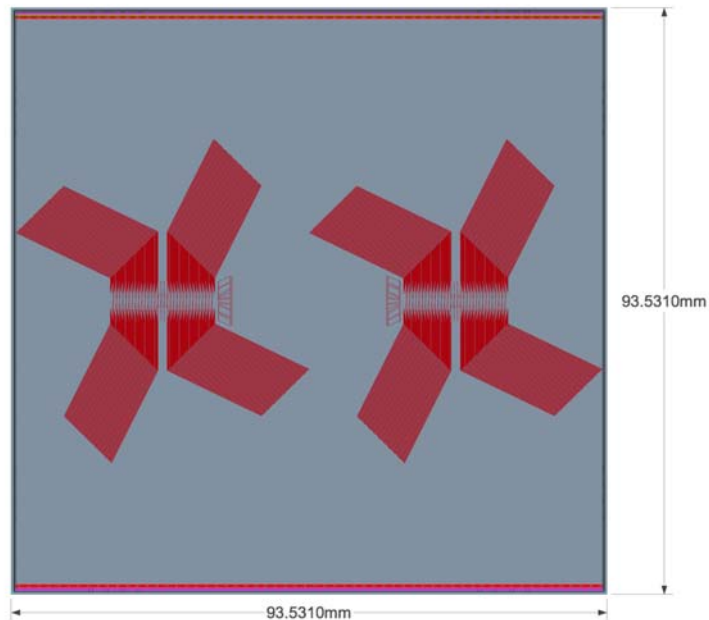


Figure 6: The design of the prototype barrel sensor showing the double-metal readout traces connecting the sense strips to the two KPIX bump-bonding arrays and the KPIX power and readout pads to wirebonding pads for the pigtail cable mounted at the center of the sensor.

3.4 Status and R&D Needs

The short module concept for SiD has many attractive features: extraordinary resolution and excellent pattern recognition capability; extreme simplicity, modularity and mass-producibility; and very low mass are all features of this design. However, only assembly and operation of full working modules can ensure that this design succeeds in all respects. This requires the development of prototype sensors, module supports and mounts, KPjX chips, cables, DAQ and power distribution, together with a sizable laboratory testing and test-beam effort. The status and plans for these efforts are described below, and the required effort is summarized in Table 3. Note that R&D for KPjX, cables, power distribution and DAQ will be covered separately in section 5.3.

We anticipate the need for two full iterations of module prototyping in both the barrel and disk, including two generations of most components and tooling. Due to the large design effort and non-recurring cost of tooling for the module supports and mounts, we are planning two sets of rapid prototypes to test and develop the support and mounting concept with the second set used as the supports for the first prototypes of both barrel and disk modules. Barrel prototyping will take place first, since tracking requirements in the barrel are already relatively well understood. Since most critical issues for the module concept do not depend upon the specific module geometry, successful completion of barrel prototyping takes precedence over the early initiation disk prototyping, allowing more time for the study of forward tracking.

Fabrication of the first barrel modules is followed immediately by a vigorous testing program including test beam running. A second test-beam run is planned for the final barrel prototypes along with the first set of disk prototypes. We expect that a second set of disk prototypes will only be necessary because the disk geometry is likely to be much more complicated and may require different types of modules. However, depending upon the final configuration of the disks, a final set of disk prototypes may not be necessary to validate the concept and could then wait until the design has been approved.

A design and specifications for prototype barrel sensors have been under development and are nearing submission to Hamamatsu Photonics Corporation for fabrication. The double-metal layer has been carefully optimized in this design to minimize and balance the performance across all channels and to mitigate potential issues with the novel readout scheme. This design should achieve S/N well in excess of 25 for all channels when read out by KPjX. In addition to the bump bonding array, standard wirebonding pads have been provided which will allow testing with the time-over-threshold chips also under development in addition to testing with well-understood readout chips from previous projects. This design also allows most of the masks to be re-used if a sensor variant without double-metal readout should be desired for fabricating longer modules.

A prototype design of the module support frame and mounting clip have been developed with input from materials manufacturers and fabricators of similar parts. A solid model of this design is being detailed and will soon be ready for submission to a rapid prototyping firm. Project collaborators have considerable experience with bump-bonding in addition to a small-scale bump-bonding facility ideal for R&D. The sensor design and specifications have benefitted greatly from this expertise and future R&D will rely heavily on maintaining capability. The

techniques required for cable attachment and wirebonding are relatively well-understood and the required facilities readily available. A preliminary concept has been developed for the full module assembly and mounting procedure with a focus on extreme simplicity and precision. In order to support the effort to assemble, test and operate full working modules and prepare for test beam running, a small but well-equipped silicon laboratory at SLAC has been designed and several pieces of key equipment have already been acquired. Execution of this plan awaits SLAC funding for preparation of an existing laboratory space as a clean area suitable for this purpose.

The first barrel sensors will be delivered in FY2007 followed by delivery of a second submission in FY2009 at a cost of approximately \$100K for each submission. Design work for the barrel sensors requires 0.25 FTE-years of a physicist and 0.5 FTE-years of a designer. Sensor probing and mechanical testing will require 0.25 FTE-years of a technician, postdoc or graduate student. Development of the disk sensors will require 1.0 FTE-year of a physicist for forward tracking studies focused specifically on the sensor layout and design, followed by the same costs and effort as the barrel sensors, with deliveries in FY2009 and FY2010.

Two sets of rapid prototypes for barrel module support and mounting during FY2007 will cost \$10K and require 0.25 FTE-year of an engineer and 0.25 FTE-year of a technician for testing. Design of the final support and mounting scheme during 2008 will require 0.5 FTE-years of an engineer and \$150K for the design and fabrication of tooling and the production of a small number of supports and mounts. Testing during FY2009 will require 0.25 FTE-years of an engineer and 0.25 FTE-years of a technician. The costs for developing support and mounts for the disk modules are expected to be the same, with rapid prototyping during FY2008 and FY2009, and final prototyping taking place during FY2010 if the differentiation between the barrel and disk modules justifies this step.

The first barrel module prototype will be assembled and tested during FY2008. Fixtures and assembly tooling require 0.25 FTE-years of an engineer and \$10K for fabrication, 0.25 FTE-years of a technician for assembly and test setup. We estimate that \$25K will be required in FY2007 to assemble the DAQ and a complete laser test-stand to support the module testing efforts and expect that 0.5 FTE-years of a physicist and 0.5 FTE-years of a postdoc or grad student will be needed to test and characterize these modules. The resources for assembly of the second set of barrel prototypes will be similar. However, the effort required to fully test of order 10 modules will be roughly double the testing effort for the first prototypes. The costs and efforts for assembly and testing of the two sets of disk module prototypes from FY2009 through early FY2011 is estimated to be similar.

Mechanical design for the first test-beam run will require an a 0.25 FTE of an engineer and \$5K for fabrication and 0.25 FTE-years of a technician for assembly of the test-beam setup in FY2008. We estimate 0.25 FTE-years of a postdoc or student for test-beam specific software, and 1.0 FTE-year of a postdoc or graduate student for data analysis. Costs and effort for the second, more complicated test beam setup are expected to be roughly 50% larger in FY2009 and FY2010. Power distribution and DAQ costs for these test beam runs are covered separately in section 5.3.

| Resource | 2007 | 2008 | 2009 | 2010 | 2011 | Totals |
|-------------|------|------|------|------|------|--------|
| M&S | 135K | 175K | 230K | 265K | - | 805K |
| Staff | 1.0 | 1.0 | 0.75 | 0.75 | 0.5 | 4.0 |
| Postdocs | - | 0.5 | 0.5 | 0.5 | 0.75 | 2.25 |
| Elec. Eng. | - | - | - | - | - | - |
| Mech. Eng | 0.5 | 1.25 | 1.0 | 0.25 | - | 3.0 |
| Students | - | 1.25 | 1.25 | 0.75 | 0.5 | 3.75 |
| Technicians | 0.25 | 0.5 | 1.0 | 0.75 | 0.25 | 2.75 |

Table 3: Costs and effort for prototyping and testing barrel and disk sensor modules, including the assembly, operation and analysis of two test beam runs. Excluded are KPiX, cable, DAQ and power supply R&D, covered separately later.

3.5 Thin Silicon

Material minimization in the ILC detectors is important both to achieve excellent impact parameter resolution and for the precise measurement of low momentum tracks. Material minimization therefore impacts silicon pixels that provide precise space points near the interaction region, a silicon microstrip tracker further from the primary interaction region, and the measurement of tracks at small angle in the forward region.

The Purdue group is investigating the potential of thin silicon for ILC applications. In 2004 using DoE ADR funding, we procured silicon strip sensors from MICRON Ltd. in the following thicknesses: 150 μm , 200 μm , and 300 μm produced on 4 inch wafers. Since most silicon detectors to date have been built with 300 μm thick sensors, the 300 μm sensors provide a reference point. The sensors were manufactured on wafers that had been thinned before processing using the masks developed for the silicon layer mounted on the CDF beam pipe. Each sensor is 7.84 cm long, 0.843 cm wide, with 256 microstrips designed to be connected to 128 channels of readout electronics. In 2004 we also received double-sided silicon n^+ on n pixel sensors on 6 inch wafers. These wafers are 200 and 300 μm thick. Each n^+ pixel is 100 μm \times 150 μm in size, matching the PSI46 0.25 μm readout chip developed for the CMS pixel detector at the LHC.

We have carefully evaluated the DC performance of the thin silicon strip sensors including measurements of the capacitance to ground and the leakage current as a function of the bias voltage. Strip-by-strip scans were also performed to measure the leakage current (I_{leak}), the interstrip capacitance (C_{IS}), the coupling capacitance (C_{C}), the interstrip resistance (R_{IS}) and bias resistance (R_{bias}) at a bias voltage above the depletion voltage. The results are summarized in Table 4. The depletion voltage of the sensors was found to scale with the thickness, as expected. The 300 μm thick sensors have depletion voltages between 85 V and 105 V. The depletion voltage decreases to 30 V and 15 V for 200 μm and 150 μm sensors respectively. The leakage current is usually dominated by the bulk current and it is expected to increase with the sensor thickness. The current of the 150 μm thick sensors satisfy the required specifications including $I_{\text{leak}} < 50 \text{ nA/cm}^2$ at a bias voltage equal to twice the depletion voltage. At larger V_{bias} the current is larger and similar to that measured in 300 μm devices indicating that the leakage current at larger bias voltage is dominated by thickness independent sources such as surface current. Strip-by-strip scans verified that sensors pass the specification: $C_{\text{C}} > 10 \text{ pF/cm}$ and $C_{\text{IS}} < 1.2 \text{ pF/cm}$. The bias resistance of the 200 and 150 μm thick sensors was within the specification of $R_{\text{bias}} = 1.5 \pm 0.5 \text{ M}\Omega$. It was below specifications for the 300 μm thick sensors. In summary all seven 150 μm thick sensors pass the specifications we had set. These results, summarized in Table 4, confirm that thin detector processing can be successfully achieved. The measurements of the capacitance and resistance indicate that the resolution performance should not be compromised by reducing the sensor's thickness.

The Purdue group also measured the S/N performance of the sensors using the SVX4 chip developed for run IIb of the Tevatron. This is an essential step to fully evaluate the feasibility of thin sensors for the ILC. In a silicon detector, the signal, S, for a charged particle depends on the path length the particle traverses in the silicon and so S is inversely proportional to the thickness. With currently available electronics the noise, N, is expected to be low enough that reducing the silicon thickness from 300 μm to 200 μm would still allow a S/N above 15. For example, the SVX4 chip has a noise of 900 electrons for a capacitive load of 20 pF while the most probable signal for a 200 μm sensor is 14,440 electrons, yielding a S/N of 16. However, in thin silicon sensors there is also an increased capacitive coupling between the two sides of the sensor, which might increase the noise, and it is important to determine if this is indeed the case

| | $I_{\text{leak}}(@ V=2V_{\text{dep}})$ | C_{C} | C_{IS} | R_{IS} | R_{Bias} |
|----------------|---|--------------------|----------------------|-----------------|--|
| specifications | Grade A <50nA/cm ² Grade B <4 μ A/cm ² | >10 pF/cm | <1.2 pF/cm | >1 G Ω | 1.5 \pm 0.5 M Ω <10% variation |
| 300 | 3 Grade A 2 Grade B | 12 \pm 0.9 pF/cm | 0.9 \pm 0.03 pF/cm | >1 G Ω | 0.5 \pm 0.2 M Ω <5% variation |
| 200 | 3 Grade A | 17 \pm 1.7 pF/cm | 0.5 \pm 0.05 | >10 G Ω | 1.8 \pm 0.1 M Ω |

| | | | | | |
|-----|-----------|--------------------|--------------------------|------------------|---|
| | 2 Grade B | | pF/cm | | <10% variation |
| 100 | 7 Grade A | 16 ± 1.3 pF/cm | 0.62 ± 0.03 pF/cm | >10 G Ω | 1.8 ± 0.1 M Ω <10% variation |

Table 4: Comparison of DC characteristics of 300, 200 and 150 μm thick sensors measured at Purdue University. We follow the same notation used in the text with leakage current (I_{leak}), interstrip capacitance (C_{IS}), coupling capacitance (C_C), interstrip resistance (R_{IS}) and bias resistance (R_{bias}).

The experimental setup for the S/N measurements used a laser illuminating a microstrip sensor wire-bonded to the SVX4 readout chip connected to a PTA/PMC based DAQ system developed for Run IIb of the Tevatron. A custom made printed circuit board hosts a SVX4 ASIC and a sensor. We focused the laser on the sensor surface and scan across the surface. Initially we locate the laser between two strips to maximize the charge collection. Note that a 4 fC charge corresponds to a Minimum Ionizing Particle (MIP) for a 300 micron thick silicon sensor and about 25,000 electrons. From the slope of the gain scan curve, we determine that ~ 30 ADC counts correspond to a MIP. In Figure 7 we show the charge collected from the laser pulse as a function of voltage for 300 μm and 150 μm sensors. In both cases the charge is normalized to that collected with the 300 μm sensor at 100V.

The noise in each channel is estimated from the Gaussian dispersion of the pedestal for that channel. In our set-up, common mode noise dominates because the sensor hybrid is not grounded. At a future date, when proper shielding is installed, we expect the common mode noise to be significantly reduced. The differential noise is determined by subtracting the common mode noise. The total signal was defined as the sum of the charge in the hit strips after a pedestal is subtracted. The bias voltage was set to 100 V which is above depletion voltage for all sensors. The error on the signal is typically less than 1% and the error on the noise is typically less than 3%.

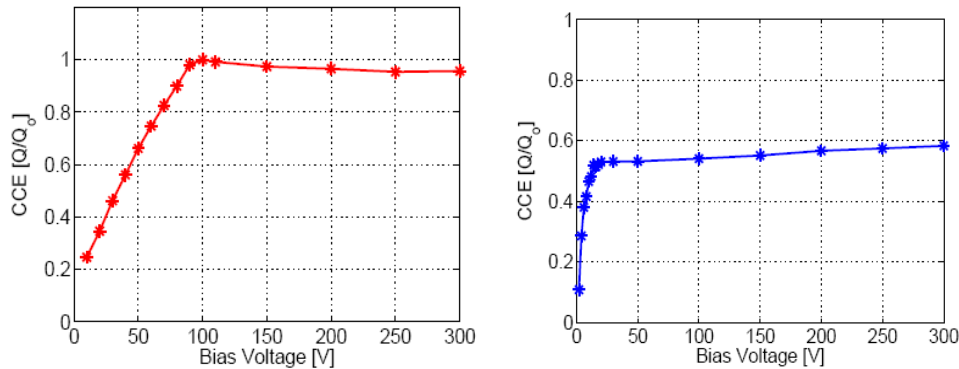


Figure 7: Charge collection efficiency for a 300 μm (left) and 150 μm (right) thick sensors. In both cases the charge is normalized to that collected with the 300 μm sensor at 100V.

The signal-to-noise (S/N) ratios are about 10.5, 8 and 5.4 for 300, 200 and 150 μm sensors respectively. The noise for all sensors is about 2 ADC counts and is independent of the thickness in agreement with the DC characterization. The S/N is about a factor of two smaller for 150 μm sensors than for 300 μm sensors. This is consistent with expectations and demonstrates the utility of thin silicon in this application. However the S/N performance is disappointing even for the 300 μm thick sensors. Studies of the SVX4 ROC indicate that the noise of this chip is $N=400+45C$, where C is the capacitance of a strip to ground. For our sensors the total capacitance is about 4 pF and therefore the expected noise is about 570 electrons. Assuming a most probable charge of 72e-h pairs/ μm we expected a S/N of about 38, 25 and 19 for 300, 200 and 150 μm thick sensors. The Purdue group is investigating the discrepancy between the expectations and the results of the S/N measurement. One possibility is that less charge was injected than we have estimated.

In the next year Purdue proposes to

- 1) Improve our understanding of the S/N with the current setup
- 2) Initiate radiation hardness (X-ray irradiation) studies using the Cobalt 60 source available at Purdue University.
- 3) Characterize thin sensors with the KPiX chip developed for the ILC. and study the S/N ratio with the laser. For this study we would like again to compare the performance of sensors of different thicknesses.
- 4) Collaborate closely with other SiD groups to develop and evaluate possible support structures for forward region sensors.

4 SENSOR TESTING

4.1 General Requirements

To ensure high quality of the silicon sensors, a series of quality assurance (QA) tests will be performed. A brief summary of the tests foreseen are included in this section. Quality assurance will be a collaborative effort and is shared among different institutions. The institutions participating in the QA program are the University of New Mexico, SLAC and Fermilab. The following sections describe the tests that will be performed by the testing centers. All electrical tests will be carried out in a temperature and humidity controlled environment, with the sensors placed in a light tight dark box. The equipment necessary to perform these measurements is summarized in Table 5.

| | |
|----------------------------------|--------------------------------------|
| Dark Box | Mechanical Shop |
| Keithley 237 | Keithley Instruments |
| Rack Mounting kit | Keithley Instruments |
| HP LCR 4284A | Agilent |
| Cable option | Agilent |
| Test Leads | Agilent |
| Isolation Vibration Table | Kinetic Systems 1201-05-11 |
| Probe Station | Alessi Rel – 6100, Cascade microtech |
| Guard Box | self made |
| Storage | Terra Universal Dessicator |

Table 5: Sensor testing equipment.

The following tasks will take place at the testing centers:

- Initial registration of sensors
- Visual inspection
- Sensor characterizations on sub-samples, as described in this document
- Shipping and handling of the rejects which are returned to the supplier
- Overall monitoring of the QA program
- Final acceptance and grading of sensors

We expect the manufacturer to perform the following tests:

- 1) Tests on each sensor
 - a) Leakage current as a function of reverse bias up to 500 V at room temperature ($T = 21 \pm 1^\circ\text{C}$) and relative humidity (RH) < 50%
 - b) Optical inspection for defects, opens, shorts and mask alignment (better than $2.5 \mu\text{m}$)
 - c) Depletion voltage measurement either by measurement of the capacitance between back-plane and the bias ring at 1 kHz frequency as a function of reverse bias, or by similar measurement performed on a test diode produced on the corresponding wafer.
- 2) Tests on each strip
 - a) Capacitance value measurement and pinhole determination
 - b) Leakage current at Full Depletion Voltage (FDV) and Room Temperature (RT)
 - c) The total number of not working channels must not exceed 1%. Non-working channels are defined as:
 - i) Pinholes – current through capacitor >10 nA at 80 V and RT
 - ii) Short – coupling capacitor >1.2 times the typical value
 - iii) Open – coupling capacitor <0.8 times the typical value
 - iv) Leakage current above 10 nA/strip at FDV and RT
 - v) Strips with bias and interstrip resistance values out of our specifications
- 3) Tests on test structure
 - a) Poly-resistor value
 - b) Sheet and implant resistivity
 - c) Coupling capacitor breakdown voltage

The QA program for silicon sensors consists of four main parts:

- 1) **Key tests** are performed on every received sensor. The measurements / procedures belonging to this QA part are the most important ones to effectively determine the basic sensor parameters. They include
 - a) Visual inspection
 - b) I-V measurement

- c) C-V measurement
 - d) The sensor subset tests consist of the following measurements:
 - i) Leakage current stability I(t)
 - ii) Full Strip Test (AC scan)
 - iii) Strip leakage current test (DC-scan)
- 2) The **diagnostic tests** will be performed on all sensor as well. The diagnostic tests measure in much more detail complex electrical parameters in order to get a deeper insight into the sensor qualities and to monitor the production process. The diagnostic tests consist of the following measurements:
- a) Polysilicon resistor measurements
 - b) Strip and interstrip capacitance
 - c) Metal series resistance
 - d) Implant sheet resistance
 - e) Flat band voltage measurements on MOS test structure (if available)
 - f) Interstrip resistance
 - g) Coupling capacitor and coupling capacitor breakdown value on test structure
- 3) The **mechanical test** measurements are introduced to verify the mechanical tolerances on the wafers. They will be routinely performed on 25% of the delivered sensors per batch. Tests will check for
- a) Sensor thickness
 - b) Sensor warp
 - c) Sensor cut dimensions and cutting accuracy

5 FRONT-END READOUT

5.1 Introduction

The baseline design calls for readout of the silicon sensors using the KPiX chip, which is being developed at SLAC for use in the tracker, as well as the silicon-tungsten electromagnetic calorimeter (ECAL). Two alternatives to the KPiX chip are also being pursued: a Time-over-Threshold readout and a readout employing charge division. Each option and the corresponding R&D will be explained in the following sections.

5.2 KPiX Readout Chip

The central component of the novel readout scheme proposed for SiD is the KPiX readout chip. Under development at SLAC for use in both the SiD tracker and calorimeter, KPiX has two key capabilities that enable the simple, low-mass module design previously described. First, KPiX is designed for pulsed power, starving the power-hungry front end for current between bunch trains. This reduces the power consumption to 20 mW average for a 1024-channel KPiX chip, or 40 mW for a single-sided module. Second, KPiX has four time-stamped analog buffers per channel that store signals from the detector until the inter-train period for digitization and readout. As a result, the only digital activities on KPiX during the bunch train are a synchronous LVDS clock and individual comparators firing when a channel crosses the readout thresholds. This low-noise mode of operation during the bunch train allows KPiX to be mounted directly to the sensor without inducing large RF pickup on the strips. An individual cell of KPiX is shown in Figure 8.

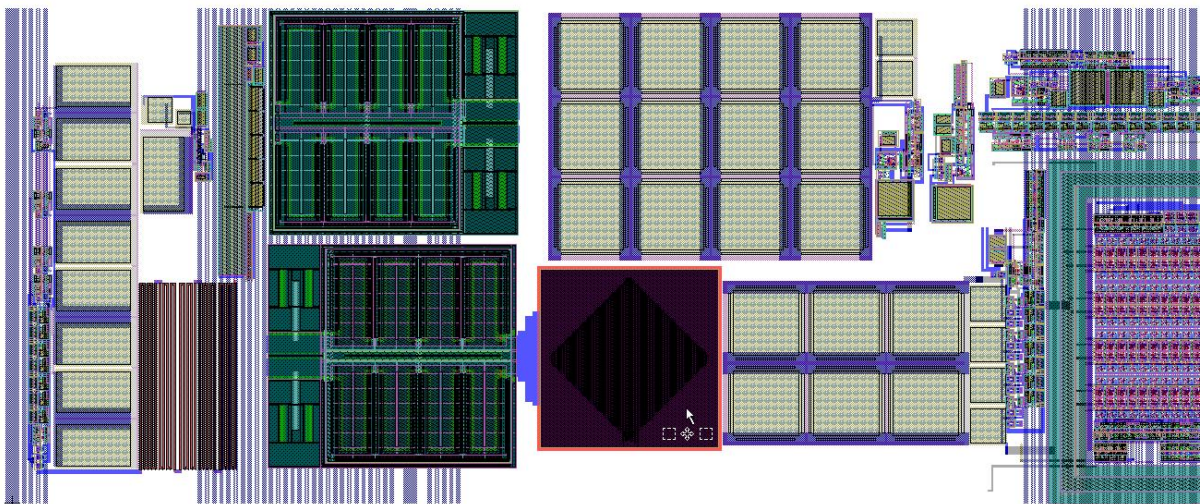


Figure 8: An individual cell of the KPiX readout chip

This design includes a number of elements that require R&D. Most importantly, the simple concepts for both the tracker and the calorimeter rely upon the unique attributes of the chip design. Only prototyping tracker and calorimeter modules with KPix can prove that these pioneering designs can be realized. Further, it must be shown that the power-pulsing scheme works as designed, reducing power consumption by an acceptable factor without negatively impacting stable operation. Since the pixellated layout places the analog and digital sections in close proximity, it must be demonstrated that the excellent noise performance needed for the tracker can be assured. Finally, with 1024 channels and a great deal of functionality in each cell, KPix is simply a very complicated ASIC and successful fabrication must be established.

5.2.1 Signal-to-noise Ratio

Signal to noise ratio (S/N) is an important parameter that determines both the single-hit efficiency and single hit resolution of the tracker². Single-hit efficiency is uniformly excellent above $S/N \approx 12$, but single-hit resolution continues to improve up to $S/N \approx 20$. In particular, the floating strip arrangement of the barrel sensors has approximately 30% better resolution at $S/N=20$ than at $S/N=12$. It is therefore important to achieve high S/N in order to have the most precise momentum measurements at high momenta.

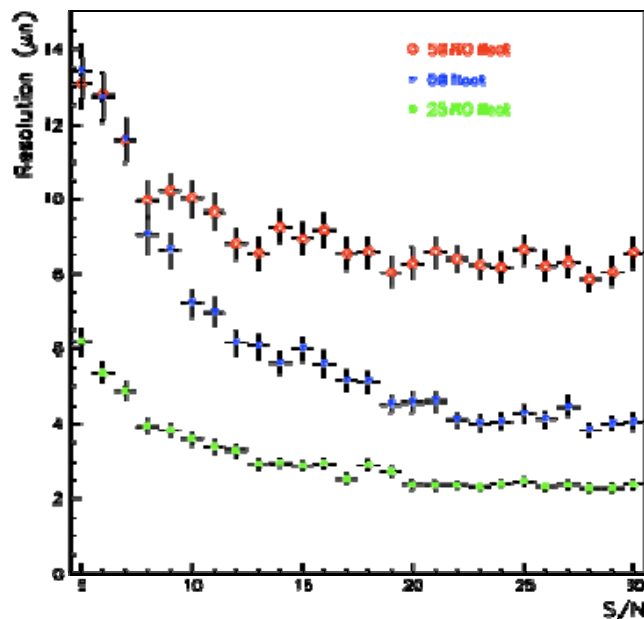


Figure 9: Single-hit resolution as a function of S/N for three strip configurations. For 50-micron pitch and 25-micron pitch with every strip read out (red and green respectively) there is little improvement above $S/N=15$. Addition of a floating, intermediate strip to sensors with 50-micron readout pitch (blue) improves resolution markedly at high S/N with no additional readout.

² Signal here refers to the charge on a cluster of strips with a one-MIP signal resulting from the passage of a single-particle at normal incidence: in 300 microns of silicon, roughly 22,000 electrons distributed over one to three strips. Noise is the single-strip noise: the equivalent noise charge (ENC) per strip.

The design goal for the SiD tracker has been conservatively placed at $S/N > 25$. We have considered several contributions to the total noise for KPiX readout:

- Noise in the front end due to capacitive load.
- Noise due to the series resistance of the aluminum traces of the silicon sensors.
- Shot noise from detector leakage current.
- Thermal noise due to the finite value of the bias resistor.

This noise estimate agrees with measurements using the GLAST Tracker Front End chip from which the front end KPiX descends and provides a design envelope for the silicon sensors to ensure that we achieve the S/N goal:

- The capacitance of all readout strips shall be less than 40 pF.
- The series resistance of all readout strips shall be less than 500 Ohms.
- The leakage current shall be less than 10 nA/strip.
- The bias resistance for all strips shall be more than 4 MOhms.

Since the prototype sensor design exceeds all of these specifications by a significant margin, it will be possible to consider thinning the silicon or designing longer modules if KPiX delivers noise performance according to its fundamental design. However, KPiX is still in early phases of development and this performance must yet be established. In particular, the pixellated design of KPiX creates challenges for effectively isolating the analog and digital functions of the chip and additional noise may be encountered. Furthermore, strips that couple to the chip, cable or double-metal KPiX traces may experience some irreducible, additional noise.

5.2.2 Status and R&D Needs

The KPiX chip has been under development at SLAC since 2004 for use in the SiD calorimeter with development of KPiX as a tracker chip beginning in 2005. KPiX is a large chip, roughly 8mmX18mm so fabrication of full-sized KPiX chips for R&D is a major expense. For this reason, an inexpensive, reduced-size version of KPiX with 64 channels (2X32 instead of 32X32) has been used for prototyping and the fourth generation of this chip, KPiX64-4, has just been received at SLAC for testing.

Although development of KPiX has previously been funded entirely under SiD Ecal R&D, the KPiX effort has broadened considerably to include the HCal as well as the tracker: the efficiencies of using KPiX based-readout in many SiD subsystems provide cost savings throughout the project due to common power and DAQ needs. With this transformation, we anticipate that future KPiX development will be shared by the tracker and calorimeter efforts at SLAC, and significant tracker-specific KPiX R&D has already commenced. The addition of nearest-neighbor readout capability for the tracker and simulation studies to ensure the excellent noise performance demanded by the tracker application are two examples of this work.

The KPiX schedule is tied closely to the MOSIS TSMC 0.25 micron submission schedule. One more submission of KPiX64 is planned for April 2007 before a submission of a 128-channel chip in June to study any issues that scale with the chip size. After final testing and qualification, the full sized KPiX-1 will be submitted in late August and delivered before the end of FY2007. The

cost to the tracker project of these submissions will be 83K, 0.25 FTE of an electronics engineer for design and 0.25 FTE each of a physicist, a technician and a graduate student for testing in FY2007. After building the first modules with KPiX-1 and studying the full-sized chip in detail in both the laboratory and test beams, we anticipate submission of a second version, KPiX-2 before the end of FY2008, which will be used for the final barrel module prototypes and the disk module prototypes, including the second test beam run. This work will require a similar effort in FY2008 for design and testing, and the cost of the final submission is estimated at \$50K. The effort is summarized in Table 6.

| Resource | 2007 | 2008 | 2009 | 2010 | 2011 | Totals |
|-------------|------|------|------|------|------|--------|
| M&S | 83K | 50K | - | - | - | 133K |
| Staff | 0.25 | 0.25 | - | - | - | 0.5 |
| Postdocs | - | - | - | - | - | - |
| Elec. Eng. | 0.25 | 0.25 | - | - | - | 0.5 |
| Mech. Eng | - | - | - | - | - | - |
| Students | 0.25 | 0.25 | - | - | - | 0.5 |
| Technicians | 0.25 | 0.25 | - | - | - | 0.5 |

Table 6: Costs and effort for half of the KPiX R&D effort. The other half is to be borne by the ECal R&D effort.

5.3 Power Distribution and DAQ

Average power requirements for the SiD tracker are modest, less than 500 Watts for the entire tracker. However, power cycling means that peak power will be larger by approximately two orders of magnitude. As a result, power supplies and the power distribution system are not trivial components of the overall design and will require significant R&D to ensure adequate and stable power during collisions. The DAQ required for individual KPiX operation is similarly modest: the USB-based DAQ needed for testing KPiX and individual modules is simple and can be fabricated with little effort and expense. However, in contrast to power distribution, the R&D needed to scale the DAQ up for readout of the entire tracker is minimal.

For operation of the large number of modules in the final detector, power and readout distribution boards, called concentrators, will be mounted at the ends of each barrel. Each board

will service up to 20 modules, providing power, distributing control signals and concentrating data for readout. Electronic DC-to-DC converters reduce the mass of cables between the power supplies and these boards by bringing in power to the concentrators at higher voltage/lower current and stepping the voltage down to supply current to the modules. Optical transceivers convert optical control and readout signals for the external DAQ to/from digital signals for KPiX.

Charge pump DC-to-DC converters that are operable in the large magnetic field of SiD are available but generally operate with smaller step-downs typical of applications in laptops and other mobile devices. Although design of the required circuitry seems feasible, the large EMI and ripple associated with charge pump converters are likely to be critical issues here and may present design challenges to creating a low-noise environment inside the tracker. Furthermore, these devices are typically capable of only modest supply currents, so providing the large instantaneous currents required during acquisition could present an obstacle to implementing this scheme. An alternative to this approach is the kind of serial powering scheme being investigated for the vertex detectors, which also have significant obstacles to overcome. Since this scheme is important to minimizing mass in the outer portion of the barrel-disk overlap where external power cables are routed, understanding and resolving these issues with R&D culminating in the successful operation of modules with such a supply is critical.

In contrast, the capability and efficiency of off-the-shelf optical transceivers has exploded due to the emergence of high-speed computer networking. Current off-the-shelf optical transceivers are small enough, fast enough and consume little enough power for our application so that only modest testing and qualification will be required to ensure their usability in the SiD tracker.

5.3.1 Status and R&D Needs

The design of the power and readout distribution system for the SiD tracker is currently little more than a concept. The concentrator boards have a natural location at the ends of the barrels that maximizes accessibility and simplifies the process of module mounting and overall tracker assembly. We have investigated commercial optical transceivers and found that standard off-the-shelf components meet all of our power and rate requirements. Similar investigation of DC-DC converters indicates that a custom design for this circuitry will be required. Meanwhile, DAQ and power supplies capable of operating individual KPiX chips are relatively simple and have been available and operating at SLAC for some time.

We anticipate that R&D on the large-scale power and readout system for the SiD tracker will naturally coalesce around the test beam activities where these components will be required. A first prototype including power supplies and standard KPiX DAQ, but without DC-DC converters or optical transceivers will be assembled for the first test-beam run in FY2008. This will be followed in FY2008 and FY2009 by assembly of a prototype concentrator board complete with optical readout and DC-DC converted power for operation of the second test-beam setup in FY2010. The cost of components is estimated at 25K, with design, assembly and testing requiring 0.75 FTE-years of an electronics engineer, 0.75 FTE-years of a technician and 0.5 FTE-years of a graduate student. The effort is summarize in Table 7.

| Resource | 2007 | 2008 | 2009 | 2010 | 2011 | Totals |
|-------------|------|------|------|------|------|--------|
| M&S | - | 10K | 15K | - | - | 25K |
| Staff | - | - | - | - | - | - |
| Postdocs | - | - | - | - | - | - |
| Elec. Eng. | 0.25 | 0.25 | 0.25 | - | - | 0.75 |
| Mech. Eng | - | - | - | - | - | - |
| Students | - | - | 0.5 | - | - | 0.5 |
| Technicians | 0.25 | - | 0.5 | - | - | 0.75 |

Table 7: Costs and effort for R&D on power distribution and DAQ, including design and fabrication for operation of both test-beam runs.

5.4 Time-over-Threshold Readout

5.4.1 Introduction

Time-over-Threshold readout is being pursued by Bruce Schumm at the University of California at Santa Cruz (UCSC). An alternative to the KP1X chip, the Santa Cruz Institute for Particle Physics (SCIPP) Long-Shaping Time Front-End (LSTFE) ASIC is based on a dual time-over-threshold readout of silicon microstrips. The LSTFE ASIC features a long shaping-time, low-noise readout that can be used to readout long ($> 1\text{m}$) daisy-chained sensor ladders, or to read out short ($\sim 10\text{ cm}$) modules with ultra-high signal-to-noise. Employing power cycling with a turn-on time of less than 1 msec, the chip will consume an average power of less than $10\ \mu\text{W}$ per channel. Analog information is provided by recording the time spent above the threshold of a comparator set at a small fraction (approximately 15%) of minimum ionizing. To avoid unacceptable noise occupancy, a second threshold (approximately 30% of minimum ionizing) is applied to each channel. Digital logic currently under development on an FPGA, but eventually to be incorporated into the LSTFE ASIC, will enable the readout of the lower threshold comparator only for channels close in time and space to a channel exhibiting a high threshold crossing. Simulation indicates that this will limit the noise occupancy to less than 0.1% even for ladders of length greater than 1.5m. Simulation also suggests that the accuracy of the centroid reconstruction is limited by the statistics of the deposition process, and is not compromised by the relatively crude measurement provided by time-over-threshold. The LSTFE readout is

expected to provide point resolution of better than $7\ \mu\text{m}$ for ladders in excess of 1.5m, and to do somewhat better for shorter ladders.

The LSTFE architecture will allow analog information to be accumulated and stored in a digital FIFO in real time, with the hit repetition rate limited only by the restoration of the amplified signal to baseline. Thus, the LSTFE design is particularly well tailored to use in the forward region, where background occupancy will be relatively high.

5.4.2 R&D Needed

Much of the functionality of the LSTFE approach is working with the initial prototype, although the turn-on time reduces to 1 msec only with the injection of a small ($< 1\ \text{nA}$) DC current into the front end of the pre-amplifier. A second prototype, the LSTFE-2, is under development at SCIPP, and is expected to be submitted in April 2007. This second prototype chip will incorporate a design that will eliminate the need for injected charge, and will incorporate further optimization of the noise performance, return-to-baseline, channel-to-channel matching, and dynamic range. Efforts are already beginning to turn towards the development of the digital architecture on the FPGA, and the design and construction of a long ladder, to be read out by the LSTFE-2 and digital FPGA, for a testbeam run (to be conducted in coordination with the SiLC testbeam program) in late 2007. The primary goal of this testbeam run will be to demonstrate the efficiency and resolution of the system, as well as to probe the dependence of the performance on the entrance angle of the track.

After the test beam run, a third version (LSTFE-3) of the chip will be developed, with relatively minor changes relative to the LSTFE-2 that will be geared towards use in the forward system, or the use of shorter ladders in the central region (primarily a re-optimization of the shaping time and noise characteristics for use with shorter strips, with attention to the rate capability). A second test beam run, most likely in early 2009, will test the performance of the LSTFE-3 chip.

As preparations are getting underway for the LSTFE-3 test run, two additional development threads will be started: that of the distribution scheme for the readout system power, and the optoelectronic data transmission scheme. The latter of these will be done in collaboration with SCIPP engineering faculty, who has substantial background in the development and application of optoelectronic technology.

5.5 Charge Division Readout

5.5.1 Introduction

Silicon strip sensors have proven to be an excellent choice for charged particle tracking, and all of the ILC detector concepts include them in their detector design. While silicon strip sensors excel at measuring position coordinates perpendicular to the strip direction, measurement of the coordinate parallel to the strip direction has proven problematic. The simplest approach, which is utilized in the SiD baseline design for the barrel tracker, is to only measure the bend ($r\text{-}\phi$)

coordinate, and utilize the detector segmentation to provide a coarse estimate of the non-bend (z) coordinate. The z coordinate can be accurately measured using a second sensor oriented with a small stereo angle, but this increases the amount of material in the tracking volume, significantly increases the detector cost, and introduces ghost hits. Double-sided detectors can provide both axial and stereo coordinate measurements on the same sensor, but have proven difficult to manufacture and handle.

A critical R&D need for the ILC is the development of silicon strip tracking detectors that can economically cover large areas while minimizing the amount of material in the tracking volume. Ideally, a single silicon sensor would provide 3D space-point measurements of charged track hits based on 2-D coordinate measurements in the sensor plane and the known position and orientation of the sensor. A new R&D effort that has recently been initiated is to develop silicon strip detectors have this capability. Our goal is to maintain the excellent position resolution traditionally available from strip detectors in the coordinate perpendicular to the strip direction, while simultaneously measuring the coordinate parallel to the strip direction using a charge division technique.

The technique of resistive charge division has been widely utilized in wire chambers. Consider a strip with a uniform resistance and capacitance per unit length. Charge deposited locally will create a voltage on the local element of capacitance, causing currents to flow in both directions. The charge will diffuse down both ends of the strip, and can be collected by low impedance amplifiers at the two ends of the strip. The fraction of the total charge collected is a function of time and the position z where the charge was deposited on the strip³:

$$Q(t, z)/Q_0 = 1 - \frac{z}{L} - \sum_{m=1}^{\infty} \frac{2}{m\pi} \sin\left(\frac{m\pi z}{l}\right) \exp\left(\frac{-m^2\pi^2}{\tau_D} t\right)$$

where Q_0 is the charge deposit and $\tau_D = RC$ is the detector time constant, R is the total resistance of the strip, and C is the total capacitance of the strip, and L is the length of the strip. For $t > \tau_D/2$, essentially all of the charge is collected from the strip and the hit position is related to the fraction of charge collected

$$Q(t > \tau_D/2, z)/Q_0 \approx 1 - \frac{z}{L}.$$

The accuracy with which the hit position can be measured is limited by the thermal noise in the detector. Since the strip has a low impedance connection at the far end, the strip acts as a parallel noise source across the amplifier input, producing a noise current density of

$$\langle i_N^2 \rangle = \frac{kT}{R}$$

³ R.B. Owen and M.L. Awcock, IEEE Trans. Nucl. Sci. **15**, 290 (1968).

at the amplifier input. Radeka⁴ has shown that with filtering optimized for high S/N and short resolving time, the equivalent noise charge is

$$\langle ENC^2 \rangle \approx 1.17 \frac{kT}{R} \tau_D = 1.17kTC .$$

Note that for optimal filtering, the charge noise is independent of the strip resistance, and only depends on the strip capacitance.

Since the charge noise on the two ends of the strip is anti-correlated, the total measured charge Q_0 is assumed to have negligible noise. Thus, the position resolution is given by

$$\frac{\sigma_z}{L} = \frac{\sqrt{1.17kTC}}{Q_0} .$$

For a strip capacitance of 10 pF, a strip length of 100 mm, and a charge deposition of 25000 electrons, the position resolution is predicted to be 5.5 mm.

We have developed a spreadsheet model of a lumped distributed R-C circuit as a first study of the application of charge division techniques in silicon strip detectors. We assume that the detectors are DC coupled strip detectors where we use the implant resistivity to provide the charge division. The strip capacitance is assumed to be 1 pF/cm and the implant resistivity is taken to be 40 k Ω /cm. We model the amplifier inputs as being similar to the SVX4 chip developed for the CDF and DØ Run IIb upgrades, with a 0.22pF feedback capacitance and an open loop gain of 2500 giving a dynamic input capacitance of 550 pF. The fraction of charge collection versus time is shown in Figure 10 for several different positions of the charge deposition. It is seen that the charge fraction is well correlated with position at $t \sim \tau_D/2 = 2 \mu s$. Due to the finite dynamic capacitance, the charge collected will eventually equilibrate between the two ends, which explains why the charge fraction is seen to be slowly trending towards a charge fraction of 0.5 for times greater than the 2 μs charge collection time.

⁴ V. Radeka, IEEE Trans. Nucl. Sci. **21**, 51 (1974).

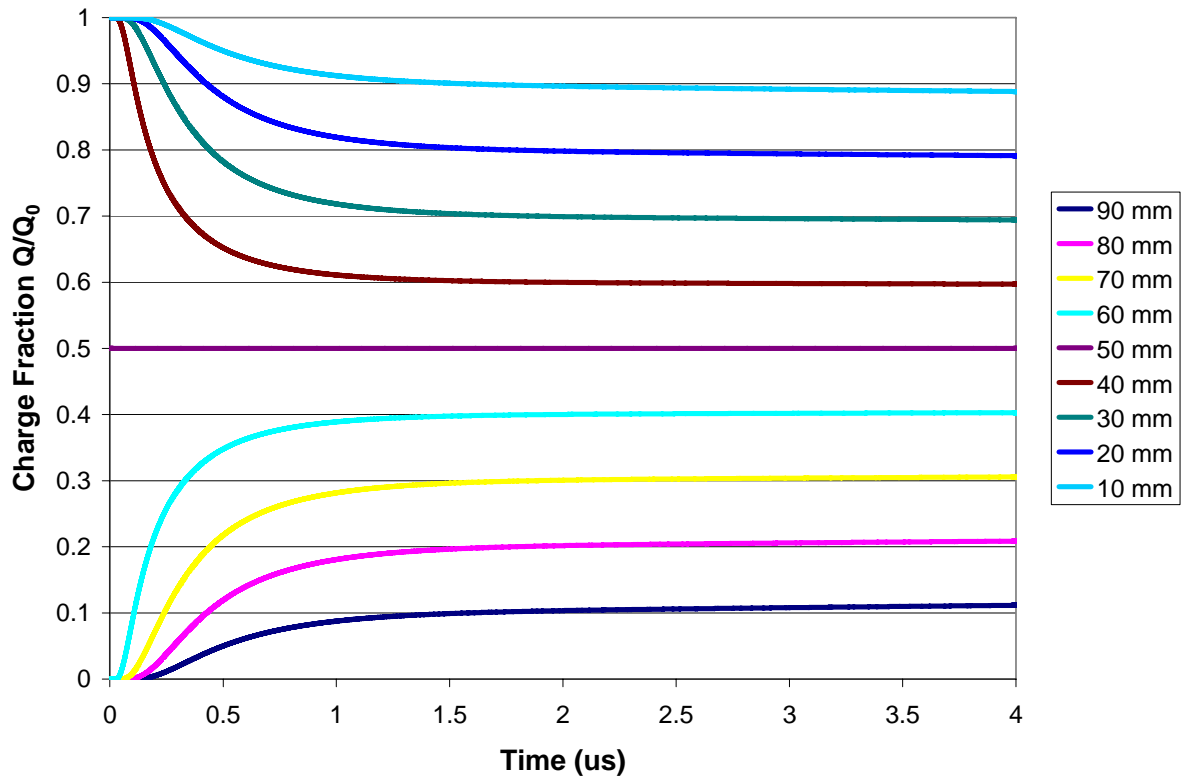


Figure 10: Fraction of charge collected on one end of the strip for various charge deposition positions.

The ultimate goal of this work is to provide sufficient resolution in the z coordinate measurement to provide useful tracking in the r - z plane for secondary vertices where there are few or no hits in the vertex detector. In this case, we must rely on the silicon strip detectors and the calorimeter for measuring the polar angle and r - z impact parameter. To illustrate the potential use of charge division readout, consider a charged track that traverses all 5 barrel layers in the SiD concept. With charge division readout, the track will have an estimated error in $\tan\lambda$ of 0.007, which can be further improved if matching hits in the calorimeter and/or vertex detector are found. We anticipate that this level of precision will significantly improve the mass resolution for K_S and Λ decays, as well as generally aiding pattern recognition in the tracker, without significantly increasing the tracker cost or amount of material.

This R&D project proposes to investigate and test the application of charge division readout to silicon strip detectors. This effort includes:

- Simulation studies of the electrical performance of sensor and readout electronics
- Design and procurement of test sensors
- Design and submission of a readout chip optimized for charge division measurements
- Characterization of the performance of the test sensor + readout electronics

Each of these projects is discussed briefly in the sections below.

5.5.2 Simulation Studies

Simulations studies of the signal and noise performance will be performed to first verify the feasibility of the charge division technique, and then to optimize the design of the sensor and readout chip.

A key parameter in the sensor design is the resistance of the strip. Using an Al strip for charge division may prove difficult because of the very short charge collection times required. At present, it appears that using the implant as the charge division strip is a better approach. For example, a 40K Ω /cm implant resistivity leads to a charge collection time $\tau_D/2 \sim 2 \mu\text{s}$ for a 10 cm long detector. We will develop a simulation model for the sensor that can be used to study how the strip resistance affects the charge division performance and determine the optimal range of strip resistance.

The performance of the front-end amplifier and shaper circuitry is expected to be critical to achieving the best possible position resolution. The front-end amplifier needs to maintain low input impedance over the appropriate frequency range, while the shaper circuit is critical to obtaining the desired low noise performance. We will use simulations to optimize the amplifier and shaper design and to measure the noise performance that can be achieved.

5.5.3 Test Sensors

A sensor submission is anticipated in late summer 2007 to test the double metal sensor design that is the baseline sensor for the SiD detector. There remains room on this wafer for additional test structures, and we plan to include a test sensor on this wafer that will allow testing the charge division technique.

5.5.4 Readout Electronics

The readout electronics are a key part of the proposed project. We plan to develop a readout chip using the TSMC 0.25 μm process that is optimized for making the charge division measurement. The key elements of this chip will be the front end amplifier and shaper circuitry, and we expect most of the engineering effort will be on developing these circuits and simulating their performance as part of the simulation studies.

5.5.5 Performance Characterization

We plan to mount the readout electronics on the test sensors and use these devices to characterize the detector performance. Key measurements include the magnitude of correlated and uncorrelated noise, position resolution along the strip direction, and position resolution perpendicular to the strip direction. If electrical, source, and laser tests are successful, we would begin planning for a beam test in the future.

6 READOUT CABLE

6.1 Introduction

Low-mass readout cables will connect tracker modules to the concentrator boards mounted at the ends of each barrel (see Figure 11). The cable design calls for quarter-ounce copper on 50 micron thick Kapton, and specifies total resistance for each power+ground pair of less than one Ohm, allowing for cables less than 1 cm in width. Due to the simplicity of KPix operation, very few traces are required: in addition to two pairs each for analog and digital power, only eight more traces are needed for digital control and readout, along with a pair for the sensor bias. This cable is divided into two components: a short “pigtail” which is glued to the module and a longer extension cable that connects the pigtail to the concentrator. This eases assembly, handling and installation of the modules and simplifies the fabrication of the cables themselves.

The pigtail is the more complicated piece, and requires the most R&D. In addition to the traces, this cable has a pair of tabs near the sensor edge for connection of the sensor bias as well as surface-mount pads for both bias and power filtering. Since this cable glues directly to the surface of the sensor, pickup and crosstalk on the underlying strips are a concern. Prototype sensor modules that prove the SiD tracker design must include realistic pigtail prototypes to ensure that any issues can be resolved.

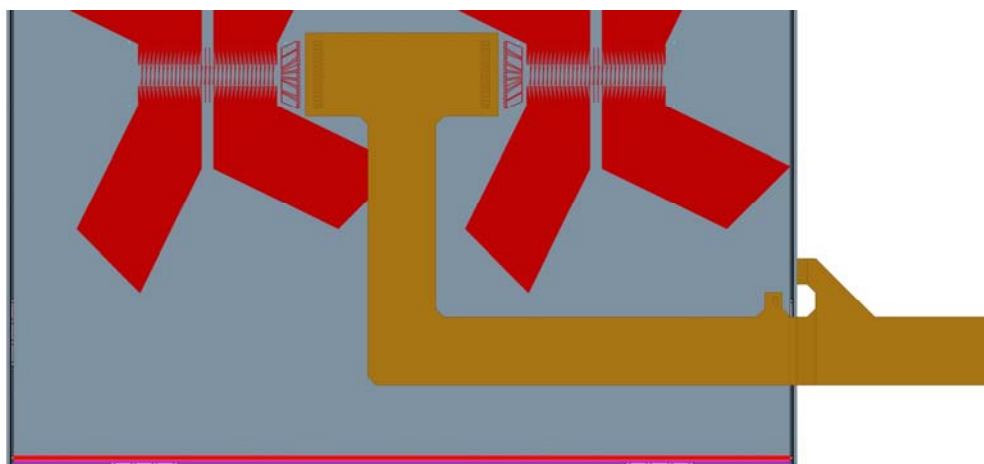


Figure 11: A drawing of the pigtail mounted to a sensor. Note the tabs for detector bias.

The extension cables are relatively simple, which is important to the feasibility of fabricating such long cables: up to 2m in length. It will be important to establish that fine-pitch cables with miniature connectors at both ends can be reliably fabricated at this length, but beyond this the extension cables present less of an R&D challenge.

6.1.1 Status and R&D Needs

We anticipate two pigtail prototypes each for both barrel and disk modules, a total of four pigtail prototypes, allowing for a unique pigtail for each module design. The extension cables are more generic, and we plan only two prototypes of the extension cable, one for the barrel and one for the disk, as these extension cables may require very different geometries due to cable routing issues. Note that while we must prove the feasibility of fabricating the extensions and operating KPiX through these long cables, their use for laboratory and test beam operation of modules will not be essential.

Pigtail R&D is intimately tied to module R&D. The barrel pigtail will be produced first, followed by the barrel extension cable. After testing, the second barrel pigtail will be produced as part of prototyping the final module design in the barrel. We anticipate the cost of prototyping the cables in both the barrel and disk to be \$40K, and that 0.5 FTE-years of a physicist, 1.5 FTE-years of an electrical engineer and 0.75 years of a graduate student will be required for the entire cable prototyping effort. This effort will be reduced somewhat if the disk design does not require production of a final module prototype as part of the R&D program. The total anticipated effort is summarized in Table 8.

| Resource | 2007 | 2008 | 2009 | 2010 | 2011 | Totals |
|-------------|------|------|------|------|------|--------|
| M&S | 30K | - | 40K | 10K | - | 80K |
| Staff | 0.25 | - | 0.25 | - | - | 0.5 |
| Postdocs | - | - | - | - | - | - |
| Elec. Eng. | 0.5 | 0.5 | 0.25 | 0.25 | - | 1.5 |
| Mech. Eng | - | - | - | - | - | - |
| Students | 0.25 | - | 0.25 | 0.25 | - | 0.75 |
| Technicians | - | - | - | - | - | - |

Table 8: Costs and effort for design, fabrication and testing of pigtail and extension cables for both barrel and disk tracker modules.

7 MECHANICAL DESIGN, STRUCTURES, AND INFRASTRUCTURE

7.1 Overview

The establishment of tracker geometry and the mechanical design of the outer tracker are challenging. Mechanical support structures must satisfy strict requirements on material mass, on precision of construction and positioning. They must allow for signal readout and cooling of the detectors, and must satisfy overall size constraints imposed by the need to install the detector within the envelope of the electromagnetic calorimeter. The overall SiD concept assumes that it should be possible to service tracker and vertex detector elements while leaving beam delivery elements and the beam pipe undisturbed.

Mechanical structures to support outer tracker sensor modules are based upon sandwiches of carbon fiber laminate – Rohacell – carbon fiber laminate. Structures of that construction were chosen to minimize the number of radiation lengths the support structures represent while providing good mechanical stability and ease of fabrication and assembly.

The cylindrical geometry of a barrel optimizes the use of carbon fiber in controlling longitudinal deflections from gravity. For barrels of lengths and diameters appropriate for the outer silicon tracker, those deflections are straight-forward to control by selecting a sensible elastic modulus and thickness for each of the two carbon fiber layers of a support cylinder. Out-of-round deflection will be controlled by adjusting the thickness of the Rohacell between the two layers of carbon fiber laminate. Openings can be cut in the Rohacell to reduce material while still maintaining its functionality as a spacer between carbon fiber layers. It is likely that openings to reduce material can be cut in the carbon fiber as well.

To limit material contributions, cooling with forced flow of dry gas has been assumed. Initial calculations indicate that a dry air flow rate of $0.035 \text{ m}^3/\text{s}$ would remove an average power of 430 watts with a 10°C rise in air temperature.

7.2 Status and R&D Needs

Spreadsheet and finite element calculations of deflections of the outermost support cylinder were made in 2004 and early 2005. The outermost cylinder was selected for those studies because, with a given cylinder wall construction, it should have the largest out-of-round distortions and because that cylinder must support the combined weight of all other barrels and disks. Loads included estimated weights of support structures, silicon, readout chips, and cables. The result was that gravitational distortions were local about locations where loads from inner barrels and disks were transferred to the outer cylinder and were limited to $\sim 13 \text{ }\mu\text{m}$. Modest reinforcement at load transfer locations should reduce distortions by roughly a factor of 2. Gravitation distortions of support cylinders of other barrels should be less than those of the outermost cylinder.

Disks were examined less completely than barrels. Disk support structures are assumed to have a construction similar to that of barrels, that is, a carbon fiber laminate – Rohacell – carbon fiber

laminated sandwich. Disks are expected to be populated with silicon modules when the disks are oriented horizontally and supported on a flat plate. The primary gravitational distortions are expected to occur as disks are rotated from a horizontal position to a vertical position during installation onto the ends of barrels. The extent to which those distortions can be addressed by installation tooling depends upon the details of disk modules and the extent to which attachment points for tooling are available.

Dimensions of barrels and disks have evolved with the tracker design. Spreadsheet and finite element calculations will be repeated once more final arrangements of sensors on disks have been developed. Those calculations will include the sizing of openings in Rohacell and carbon fiber to reduce material.

R&D costs include those necessary to demonstrate that critical mechanical design and fabrication issues have been addressed and that we are ready to move from the R&D phase to the production phase. Sufficient prototyping for those demonstrations is included. Production fixtures and associated design work are not.

We estimate that development and analysis of barrel and disk structural designs would require 0.5 FTE-year of physicist, 0.5 FTE-year of mechanical engineer, and 0.25 FTE-year designer/drafter effort per iteration. We think two iterations would be needed for a total of 1.0 FTE-year physicist, 1.0 FTE-year mechanical engineer, and 0.5 FTE-year designer/drafter.

Kinematic connections for barrels and disks are based upon a design which was previously developed for DZero silicon support structures. Reproducibility of mating of an individual connection has been demonstrated to be 2-3 μm . The number of kinematic connections and their locations remains to be determined and tested for each type of barrel and disk. We estimate that \$5K for components, \$5K for tooling, 0.25 FTE-year physicist, 0.5 FTE-year mechanical engineer, FTE-year of a designer/drafter, 0.25 FTE-year mechanical technician, and 0.15 FTE-year coordinate measuring machine operator/programmer would be needed.

The rails or equivalent which would support the tracker from the inner surface of the electromagnetic calorimeter need to be designed, as does the temporary support structure which would allow the tracker to be rolled longitudinally during servicing. Rail details depend upon the dimensions and contour of the inner surface of the electromagnetic calorimeter. The tracker mounts should incorporate the ability to make position adjustments. Ideally, mounts would not over-constrain the tracker. We estimate that \$25K for prototype components, \$25K for tooling, 0.25 FTE-year physicist, 0.25 FTE-year mechanical engineer, 0.25 FTE-year designer/drafter, 0.25 FTE-year mechanical technician, and 0.25 FTE-year CMM operator/programmer would be needed.

Mounts need to be designed to attach power conditioning and distribution boards to the rings which connect one barrel to the next. We estimate that \$5K for components, \$5K for tooling, 0.15 FTE-year physicist, 0.25 FTE-year designer/drafter, and 0.25 FTE-year mechanical technician would be needed.

The design of sensor modules for barrels needs to be finalized and the design and arrangement of sensor modules for disks needs to be developed. The designs must take into account cabling,

cooling, and the development of sufficiently reproducible mounts. We estimate that \$25K for components, \$25K for tooling, 0.75 FTE-year physicist, 1.0 FTE-year mechanical engineer, 1.0 FTE-year designer/drafter, 0.25 FTE-year mechanical technician, and 0.25 FTE-year CMM operator/programmer would be needed.

Fabrication, assembly, and handling tooling should be developed and tested. In the ideal world, procedures and tooling would be tested by fabricating at least one barrel support structure, at least one disk support structure, partially populating each of them with silicon modules, and establishing that the partial system is dimensionally stable under temperature and humidity changes and works with the full readout chain. Module alignment would be verified via some combination of coordinate measuring machine (CMM), frequency scanned interferometry, and cosmic ray measurements. Those tasks are expected to be spread over approximately two years. We anticipate that a dedicated mechanical crew, dedicated CMM operators, a mechanical engineer, and a physicist would be needed. A mandrel and associated support and handling equipment will be needed for the barrel; precision plates and associated support and handling equipment will be needed for the disk. Precision tooling will be needed for module mount installation. We estimate that \$200K for carbon fiber prepreg, \$50K for an oven, \$6K for Rohacell, \$300K for tooling, \$20K for supplies, 1.0 FTE-year physicist, 2.0 FTE-year mechanical engineer, 1.0 FTE-year designer/drafter, 4.0 FTE-year technician, and 2.0 FTE-year CMM programmer / operator would be needed.

The resin of carbon fiber prepreg normally contains additives to reduce flammability and to enhance resin properties. We will need to arrange for special carbon fiber impregnation runs and should minimize the number of batches of carbon fiber we purchase. To ensure that tracker support structures are free of high-Z materials and materials incompatible with silicon, chemical analyses and/or spectrographic analyses will be conducted on samples from each batch of carbon fiber prepreg. We also plan to make a direct measurement of the radiation length of cured prepreg samples. We estimate that \$20K for testing, 0.25 FTE-year physicist, 0.25 FTE-year mechanical engineer, and 0.1 FTE-year mechanical technician will be needed to ensure that the carbon fiber we purchase is suitable. The majority of these costs would be replicated for each batch of carbon fiber prepreg purchased.

While alternative methods for ensuring geometric accuracy may be developed, we know how to ensure sufficient accuracy in fabricating and populating support structures with the aid of a CMM. We have not received a quote for the cost of a CMM with a suitable measurement volume and precision. Based upon past purchases of smaller CMM's of suitable precision, we estimate its cost to be ~ \$500K. Such a device is needed to demonstrate that fabrication methods and tooling will produce structures of adequate precision and to measure the deflections of those structures under load. In addition, we estimate that \$20K for tooling, 0.75 FTE-year physicist, 0.5 FTE-year mechanical engineer, 0.15 FTE-year designer/drafter, 0.5 FTE-year mechanical technician, and 0.75 FTE-year of a CMM programmer/operator would be needed for CMM procurement, installation, and commissioning.

We estimate that \$10K for instrumentation equipment, \$10K for tooling, 0.5 FTE-year physicist, 0.75 FTE-year mechanical engineer, 0.15 FTE-year designer/drafter, 0.5 FTE-year mechanical technician, and 0.25 FTE-year CMM operator/programmer would be needed to verify that dry gas cooling is effective and does not generate unwanted vibrations.

R&D resources for the outer tracker mechanical design effort and the development of designs to the point at which they are ready for fabrication are summarized in Table 9. A significant portion of the resources is associated with the fabrication and testing of a barrel and a disk prototype. Those tasks would normally occur during the last two years of the R&D phase. Obligation of funds for procurement of a CMM should occur a year earlier to allow time for their fabrication, installation, and commissioning. While it may be tempting to consider shifting the purchase of a CMM to the project phase, its purchase is essential to the completion of tracker mechanical R&D.

| People (FTE-year) | | M&S (\$K) | |
|---------------------------|------|-----------------|------|
| Physicists | 4.9 | Components | 60 |
| Mechanical engineers | 6.25 | Tooling | 380 |
| Designers/drafters | 3.8 | Carbon fiber | 200 |
| Mechanical technicians | 6.1 | Rohacell | 6 |
| CMM programmers/operators | 3.65 | Oven | 50 |
| | | CMM | 500 |
| | | Testing | 20 |
| | | Supplies | 20 |
| | | Instrumentation | 10 |
| Totals | 24.7 | | 1246 |

Table 9: R&D resources for mechanical design of the outer tracker

7.3 Tracker Alignment

Tracker internal alignment and alignment with other elements of the SiD detector must take into account the type of information provided by silicon modules. In the baseline SiD concept, barrel modules provide r-phi information; disk modules and vertex detector elements provide 3-D space points. To allow initial reconstruction in the r-phi plane, traces of the barrel silicon should be sufficiently parallel to the magnetic field direction. We expect to ensure parallelism within the tracker to ± 15 microns over the length of a 100 mm long sensor. To ensure that a hit is associated with the correct strip, we expect to ensure that the silicon tracker as a unit is aligned with the magnetic field direction to ± 10 μm per 100 mm, or ± 0.33 mm over the 3.28 m length of the tracker.

Establishing and maintaining that precision sets constraints on the uniformity of the magnetic field, assumes that the field has been measured with sufficient precision, and likely requires that mounts of the outer tracker from the electromagnetic calorimeter are adjustable within a range of ± 1 mm.

The 3-D nature of measurements from disk and vertex detector elements relaxes the precision with which those elements must be aligned with the magnetic field. With the exception of small consequences associated with sensor overlaps, knowing, rather than controlling, the locations and orientations of those elements should be sufficient.

Reproducibility of the tracker after servicing sets limits on the required reproducibility of tracker mounts and guides the number of degrees of freedom each mount should provide. The excellent structural stability of the tracker under its own weight allows the tracker to be supported from the solenoid without over-constraint, thereby avoiding distortions to its shape which would be associated with geometric changes in the calorimeter. The extent to which the geometry of mounts on the calorimeter is preserved relative to the magnetic field direction determines the extent to which those mounts must be externally adjustable.

Mount details remain to be developed. In one concept of support without over-constraint, the tracker would be supported at 12 o'clock at each end. The support at one end would constrain all three transverse positions but not limit angular changes. The mount at the other end would constrain only x and y positions. Finally, a mount at one end at 6 o'clock would constrain only the x position. In practice, we are more likely to provide mounts at or below the tracker equator. We have found in the past that that reduces the effects of loads on the tracker and reduces changes in its transverse position that result from tracker servicing and detector moves. Studies to determine optimum locations of tracker mounts remain to be made.

The nominal radial clearance between tracker and beam delivery system structures is 10 mm. In the baseline design, the nominal radial clearance between outer tracker and vertex detector elements is 21 mm. Those clearances set constraints upon the precision with which alignment of detector and accelerator systems must be maintained during detector servicing and detector moves, such as those associated with a push-pull scenario.

A system to monitor clearances during a detector move appears to be essential. We will investigate whether the frequency scanned interferometer system, described in the following section, would serve that purpose. In any case, a frequency scanned interferometer system appears to be well-suited to measuring detector alignment after a move has been completed.

Once the tracker is in place, *in situ* alignment monitoring will be critical to achieving the intrinsic momentum resolutions possible. With spatial hit resolutions better than 10 microns, one will want alignment uncertainties at the level of 1 micron or better to make their contribution to momentum uncertainty negligible. This alignment precision is expected to be achieved through frequency scanned interferometry for large-scale tracker distortion and for short time scales, with minimization of residuals from fitted tracks providing module-by-module corrections good over the longer time scales required to accumulate sufficient statistics.

SiD Tracker R&D

No labor is specifically assigned to these tasks. They would primarily be done by physicists responsible for the overall tracker mechanical design and its integration with the SiD concept.

8 TRACKER REAL-TIME ALIGNMENT SYSTEM

8.1 Overview

The tracker real-time alignment R&D is carried out by the University of Michigan (K. Riles, S. Nyberg, H. Yang). The unprecedented excellent track momentum resolution needed for an ILC detector demands minimizing systematic uncertainties in subdetector relative alignments. At the same time, there is a strong desire for a very low-material tracking system. In the case of a silicon main tracker and in the case of silicon forward disks the low material budget leads to a structure that may prove difficult to keep rigid, even assuming relative precisions of a few microns are achieved in the initial assembly of the tracker system.

The short time scales on which alignment can change (e.g., from temperature fluctuations driven by variations in accelerator beam conditions, by cycling subdetector systems, or by mechanical disturbances) probably preclude reliance on traditional alignment schemes based on detected tracks, where it is assumed the alignment drifts slowly, if at all, during the time required to accumulate sufficient statistics. A system that can monitor alignment drifts "in real time" would be critical in any precise tracker and probably essential to an aggressive, low-material silicon tracker. The tradeoff one would make in the future between low material budget and rigidity will depend critically upon what a feasible alignment system permits.

All of the above considerations become magnified in the push-pull scheme, where the entire tracking system is moved repeatedly. Measuring alignment distortions during and following a move would be highly desirable.

The real-time alignment scheme envisioned for SiD is similar to the system now being commissioned for the ATLAS Detector, based on Frequency Scanned Interferometry (pioneered by the Oxford group⁵). The planned FSI system incorporates multiple interferometers fed by optical fibers from a common dual-laser source, where the laser frequencies are scanned and fringes counted, to obtain a set of absolute lengths.

8.2 Status and R&D Needs

The Michigan ILC group has set up a bench test in its laboratory to carry out R&D for an FSI system to monitor alignment of the SiD tracking system. The group has purchased, installed and commissioned the components of a self-contained FSI system that operates at optical wavelengths. These components include a Newport RS4000 optical table, two New Focus Velocity 6308 tunable lasers ($\lambda = 665\text{-}675\text{ nm}$ -- one laser is borrowed), a high-finesse (>200) Thorlabs SA200 F-P Fabry-Perot spectral analyzer, a Faraday isolator, several photodiodes with

⁵ Frequency Scanned Interferometry (FSI): The Basis of a Survey System for the ATLAS ID using fast automated remote interferometry", A.F. Fox-Murphy *et al.*, Nuc. Inst. and Meth. **A383**, 229 (1996).

amplifiers, a femto-Watt photoreceiver, retroreflectors (both prism and hollow), a National Instruments data acquisition card with 4-channel analog/digital conversion, steerable mirrors, beamsplitters, optical choppers, optical fibers, fiber couplers, a microscope for inspecting fibers, and an array of thermistors.

With this apparatus, the group has reached and extended the state of the art in precision distance measurements at DC over distance scales of a meter under laboratory-controlled conditions. Precisions better than 100 nm have been obtained, using a single tunable laser when environmental conditions are carefully controlled. Precisions under uncontrolled conditions (e.g., in the presence of air currents, temperature fluctuations) are an order of magnitude worse with single-laser measurements, but a recently commissioned dual-laser FSI system (with a 2nd laser borrowed from New Focus) that employs optical choppers to alternate the beams introduced to the interferometer by the optical fibers has allowed precisions close to 200 nm to be obtained. In this dual-laser scheme, the lasers are scanned over the same wavelength range but in opposite directions during the same short time interval. This technique, first developed by the Oxford ATLAS group, greatly mitigates systematic uncertainties due to environmental fluctuations during the scan.

A number of significant technical complications had to be overcome in implementing the dual-laser system, primarily the reduction by half of the light seen by the interferometer photodiode from each chopped beam, the reduction of useful Fabry-Perot transmission peaks, and the difficulty in handling "edge effects" at chopped-beam transitions, all leading to increased statistical uncertainties in FSI distance determinations, despite the decrease in systematic uncertainties. With refinement of the beam-chopping method and with improved analysis software, however, these hurdles were overcome and precisions of 200 nm were obtained under highly unfavorable conditions, using the dual-laser scanning technique. This achievement marked a major milestone in the ILC FSI R&D effort⁶. Progress reports on the Michigan group's alignment studies have been presented at Snowmass 2005 and at five linear collider workshops. An article concerning the single-laser benchtop FSI appeared in *Applied Optics*⁷, and an article on the dual-laser results was recently submitted to *Applied Optics*⁸.

⁶ Frequency Scanned Interferometer for ILC Tracker Alignment, H. Yang, S. Nyberg and K. Riles, Presentation at International Linear Collider Physics and Detector Workshop at Snowmass, Colorado, August 14-27, 2005, [http://gallatin.physics.lsa.umich.edu/~sim\\$hyang/talks/Snowmass-FSI-2005.pdf](http://gallatin.physics.lsa.umich.edu/~sim$hyang/talks/Snowmass-FSI-2005.pdf), to appear in the workshop proceedings.

⁷ High-precision Absolute Distance Measurement using Frequency Scanned Interferometry, H. Yang, J. Deibel, S. Nyberg and K. Riles, to appear in *Applied Optics*, <http://xxx.lanl.gov/pdf/physics/0409110>.

⁸ High-precision Absolute Distance Measurement using Dual-Laser Frequency Scanned Interferometry Under Realistic Conditions, H. Yang and K. Riles, submitted to *Applied Optics*, physics/0609187 (September 2006).

Now that several key milestones have been achieved in the FSI research and development, using off-the-shelf commercial components, the Michigan group is moving onto its next major goal, miniaturization of the FSI optical components, as preparation for building a partial prototype of the alignment system. The most important concerns are the material and mounts for the optical retroreflectors, since many of these components must be distributed well within the fiducial volume of the tracking system. The Oxford ATLAS group is using aluminum pellets which provide a simple robust solution for an LHC detector. For the ILC, however, minimizing material is more critical than at the LHC, even for the discretely distributed retroreflectors. Fortunately, the relatively low expected radiation doses in an ILC tracker permit consideration of materials unsuitable for the LHC. The Michigan group is attacking this R&D issue on several fronts. The group is testing small commercial (gridded) plastic optical retroreflectors, which are found to work well. But discussions are also underway with rapid-prototyping companies on customized designs. Another idea under preliminary investigation is silicon fabrication of retroreflector grids. Similarly, the mounts for the optical fiber pairs for delivery and return of the interferometer beams should also be light on material, although their placement primarily at the edges of the tracking system offers more tolerance.

Aside from the lightness and rigidity of the fiber mounts and retroreflectors, there are other several additional issues requiring study: robustness against misalignment of the fiber beam launchers with respect to the retroreflectors, oxidation of optical surfaces, radiation susceptibility, and temperature sensitivity.

The lasers and electronic readout systems too require R&D effort. Issues to examine include:

- Stability and absolute calibration of a fixed-length reference interferometer cavity placed near the lasers.
- Efficiency and robustness of optical splitters used to deliver the beam from a small number of lasers to many hundreds of optical fibers.
- Detection efficiency and bandwidth of the photodiodes used to measure fringes from the beam in the return fibers.
- Mechanical robustness against motion (relevant to the push-pull scheme)

In addition to these component issues, one must carry out integration tests to verify that a scaled-down FSI grid can reliably track a set of fiducial points under controlled motion. Initially this work will be carried out in a Michigan lab on a bench, but will need to be followed up with prototype silicon tracker components, ideally at a testbeam facility.

In parallel with this hardware development and commissioning, there is simulation software to be written and to be used to optimize the design of the FSI grid. Work is underway now to implement a general-purpose grid-fitting algorithm for use with variations on the SiD design. Based on these studies, a detailed FSI configuration will be designed.

It should be noted that although the FSI system outlined here is envisioned primarily as a passive real-time monitor for use after installation of the tracker, it's possible that it could prove useful in assembly too, to complement a coordinate measuring machine.

9 TRACKING SIMULATION AND PERFORMANCE

9.1 Introduction

The SiD tracker must reconstruct charged tracks with high efficiency, measure track parameters with excellent precision, provide full coverage of the available solid angle, and minimize the impact of multiple scattering and secondary interactions caused by the tracker material. Tracking simulations are a critical ingredient in optimizing the tracker design and demonstrate the robust performance required to meet ILC physics goals.

The SiD collaboration has developed an extensive software suite that is now being used to optimize the design of the detector. This includes SLIC, a GEANT4 based detector simulation and `org.lcsim`, a JAVA based software framework in which the reconstruction and analysis algorithms live. The simulation and reconstruction tools share a common geometry description, implemented in GDML. The software suite supplies convenient access to the standard event generators, both signal generators and background generators. Data is exchanged among the various programs by use of the LCIO event model and persistency library.

The tracking reconstruction software available in `org.lcsim` includes code to implement the tracking finding strategies described below. The software suite also includes vertex fitting code. The ZVtop vertex finding code is being ported to the `org.lcsim` framework and will be available soon. Another tool available within `org.lcsim` is a fast parameterized tracking simulation tool which can be used when the full power of SLIC is not required.

In the sections below, we describe the current status of the tracking simulation infrastructure, the tracking algorithms currently in use, and present results on the SiD tracking performance studies carried out to date. This is followed by a description of the R&D needed to optimize the design. As much as possible the benchmarks used for optimization of the design will be physics sensitivities, not intermediate quantities.

9.2 Tracking Simulation Infrastructure

The vertex detector and tracker designs have been incorporated in the SiD detector description that drives our simulation studies. The detector description serves as an input to SLIC, the GEANT4 based detector simulation used by SiD. Our current detector description includes both the active sensing elements, as well as our estimates of the dead material required to provide mechanical support, beam tube, readout electronics, and required services (including power and cooling). For the tracking studies reported here, the barrel sensors have been approximated by thin cylinders, while the disk sensors have been approximated by planar disks. The dead material is modeled as a cylinder, planar disk, or cone as appropriate.

We have also begun developing a fully segmented tracker description that incorporates each individual sensor as a planar device. The fully segmented tracker description will provide a highly realistic model of the tracker geometry, allowing us to study the effect of sensor overlaps and gaps, sensor mis-alignment, and more generally improve the precision of our detector

modeling. Figure 12 shows the barrel sensor layout extracted from GEANT4 for the fully segmented tracker description.

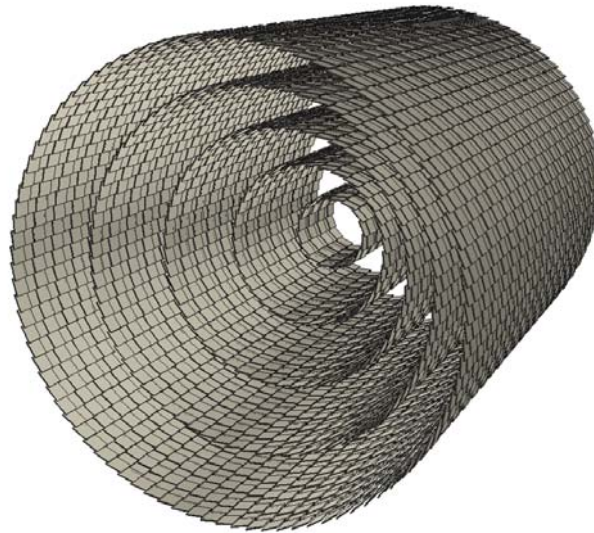


Figure 12: Barrel sensor layout in the fully segmented tracker model, as extracted from GEANT4.

Hit digitization is the process of transforming the GEANT energy deposits into strip charge depositions, and then clustering these charge depositions to form tracker hits. We have begun developing a charge deposition model. The strip sensors are assumed to be fully depleted, with the direction of the charge drift determined by the Lorentz angle. The effects of diffusion, δ -electrons, and electronics noise are included. We also account for the capacitive charge sharing between the intermediate strips and the neighboring readout strips. The full development of the digitization package is part of our R&D program. Development of the tracking software infrastructure is mainly carried out at SLAC.

9.3 Tracking Algorithms

Modern track reconstruction software typically embodies multiple track-finding algorithms. In SiD, we currently take three approaches to track finding. For tracks that originate near the IP, we use the vertex detector to identify track seeds and extend these seeds to the outer tracker. The full tracking capabilities of the SiD detector can be brought to bear on these tracks, which typically have ~ 10 precisely measured hits. Such tracks can be found with high efficiency and excellent resolution.

While the great majority of tracks originate near the IP, there are two classes of tracks that require special attention. The first is from long-lived B decays, where the B hadron decay occurs

beyond most or all of the vertex layers. We have developed a stand-alone outer tracker algorithm that can find tracks that have too few vertex detector hits to form a track seed, which is particularly relevant to this particular class of tracks. Note that the primary charged B hadrons will also leave hits in the vertex detector, further aiding their identification.

The second class of tracks requiring special attention is due to particles with long lifetimes, such as K_S and Λ . To aid in finding these tracks, we have developed a calorimeter assisted tracking algorithm that takes advantage of the fine granularity in the calorimeter to assist in track finding. This algorithm utilizes MIP stubs in the calorimeter to point back into the tracker to identify tracker hits associated with the stub.

We describe these three algorithms and their performance in more detail below. While characterizing the pattern recognition capabilities of the SiD tracker requires detailed simulations of detector response and track reconstruction algorithms, the tracker resolution is much more easily characterized. The fine granularity of the SiD tracker typically results in well separated hits with little confusion due to pattern recognition. Thus, the tracker resolution can be determined directly from the single-hit resolution, tracker geometry, and material budget.

9.3.1 Vertex Detector Based Track Seeding

The standard track finding algorithm for the SiD detector is an ‘inside-out’ track finding algorithm that takes advantage of the high precision and large number of pixels in the vertex detector to seed the track finding algorithm. For this algorithm, the pattern recognition begins in the vertex detector, and proceeds by extrapolating tracks into the main tracker.

The pattern recognition begins by selecting 3 hits in 3 different layers of the vertex detector.⁹ If a helix can be constructed from these hits, an attempt is made to associate additional hits with it. If the total number of associated hits exceeds a set threshold, the helix is considered a track candidate. For most studies a threshold of 5 hits is used. Before accepting the candidate tracks, additional criteria are applied. First, we eliminate tracks which share common hits, allowing no more than one hit in common between two different tracks. When two track candidates share more than 1 hit, we retain the candidate with the greater number of hits or, if the number of hits is identical, the better χ^2 . Another cut removes tracks associated with multiple turns of the same helix in the tracking detector. Additional criteria are imposed to reduce the number of fake tracks. By requiring a least four of the assigned hits to be in the vertex detector, the extrapolation into the main tracker is improved and false associations with noise hits are reduced. This requirement also lowers the number of track combinations that must be considered in the vertex detector, and speeds up track finding.

Because of the large number of background hits in the vertex detector, the number of hit combinations from 3 layers can be huge if we combine any hit in one layer with any combination of hits in two other layers. To reduce processing time we can impose two additional

⁹ The basic algorithm we are using here was developed a long time ago by Henry Videau for use in the PEP TPC track reconstruction and was later adapted for BaBar by Henry Lynch and Orin Dahl.

requirements: 1) the track must originate close to the interaction point (typically 1-3 cm), and 2) the transverse momentum must exceed some minimum (typically 200 MeV/c).

The vertex-seeded tracking algorithm was extensively studied in the hep.lcd framework, and the algorithm was found to be highly efficient for tracks originating near the IP (see Section 9.4). Studies using beam background events overlaid onto physics events at the pixel hit level showed the track finding algorithm to be very robust (albeit slow) in the presence of even high levels of backgrounds (a complete train, i.e. 192 beam bunch crossings, of NLC GuineaPig pairs, for instance). At the time, an alternate track finding algorithm, based on the Hough Transform, was also implemented which was shown to be very robust against backgrounds, but this approach has not been pursued. We are currently in the process of implementing the vertex-seeded algorithm in the org.lcsim framework. The Brown group is working on developing software to find seeds in the vertex detector. The Colorado group has developed software that extends vertex seeds into the outer tracker and is also developing a Kalman filter for track fitting (see next section). The Oregon group has developed a weight-matrix track fitter and performed extensive studies of tracker resolution (see Section 9.5). Future R&D includes extensive characterization of the baseline tracker performance, simulation studies to develop a more detailed design of the forward tracker, and studies of variations on the baseline tracker needed to optimize the tracker design.

9.3.2 Vertex Seeded Outer Tracking

One of the algorithms which takes these vertex detector track "seeds" and projects them into the outer barrel strip detector is the SODTrackFinder. It was developed to deal with the large outer detector occupancies when a warm Linear Collider was being considered, and has been ported to JAS3/org.lcsim framework, where it works very efficiently in the present, much lower occupancy environment. Current projects are extending this "hit-adding" pattern recognition to the forward (disk) detectors (where occupancies will once again be large), and changing out the current helix-based pattern recognition and fitting to fully Kalman-Filter based ones. These modifications should be finished in the next several months, and the final product will be supported for future physics benchmark studies.

Future R&D projects include adapting the Kalman Final Fitter to the new, much more detailed detector simulation, and investigating new algorithms, such as ones developed for the CMS detector, to improve momentum resolution for electrons (Gaussian Sum Filter techniques) and to provide purer tracks in the centers of dense jets (Deterministic Annealing Filter techniques).

9.3.3 Stand Alone Tracking in the Outer Tracker

A shortcoming of the "inside-out" approach is that ~5% of the tracks either originate beyond the inner layers of the vertex detector or have an impact parameter exceeding the 1 cm cut. These include tracks from K_S/Λ decays and long-lived heavy mesons that are at the foundation of many important physics measurements. Although the outer tracker for the SiD detector has only single-sided axial layers, we have studied the stand-alone pattern recognition capability of the outer tracker. The small size and single-bunch timing of the strip sensors, together with the very high B-field, yields very low occupancies in the outer tracker. In essence, the readout segments

are short enough that the tracker strips behave as long pixels for the purpose of pattern recognition.

The SLAC group has developed two algorithms for stand-alone tracking. A simple pattern recognition algorithm that uses circle fits to all valid three-hit combinations has been studied in the barrel tracker. We have also studied a conformal mapping technique that utilizes the 3D space points that can be reconstructed from the layer pairs in the forward tracker. While preliminary results from these algorithms are encouraging, both techniques need further R&D effort to fully develop the algorithms.

9.3.4 Calorimeter Assisted Tracking

Kansas State University¹⁰ plans to continue its development of the calorimeter assisted tracking package *Garfield*¹¹ originally written in 2004 by KSU physicists Eckhard von Toerne and Dmitry Onoprienko. *Garfield* exploits the fine segmentation of the SiD calorimeter to find calorimeter “MIP stubs” that can be used to seed an “outside-in” track-finding algorithm. This algorithm helps compensate for the relatively small number of silicon detector layers envisioned to be employed between the pixel vertex detector and the calorimeter. One set of physics implications consists of significant enhancements in the tracker’s ability to contribute to jet energy flow measurement through: (1) substantially higher K_S and Λ vertex-finding efficiency; (2) kink finding capability in the outer tracker; (3) calorimeter back-scatter track-finding capability. *Garfield* also substantially improves the SiD detector’s ability to detect possible long-lived objects predicted by some variants of supersymmetry and other models of new physics. *Garfield* was one of the first tracking algorithms implemented in the java compatible `org.lcsim` system. It has been used by a number of groups already for tracking studies.

Goals for *Garfield* development over the next three years include: (1) optimization of secondary vertex, kink, and back-scatter track finding efficiencies; (2) furthering development of *Garfield* into an easily usable tool for detector optimization by the ILC community. One optimization study that can be performed with *Garfield* is to test whether MIP stubs can be used to reduce the number of necessary z -segmentations in the outer part of the tracker, and correspondingly the number of readout modules, thus reducing the overall heat load. Another study is to investigate whether using MIP stubs can compensate for the loss of hits in the tracker that occurs in the forward direction. These are just two examples; there are many others.

Kansas State currently receives 15% salary support of post-doc Onoprienko, plus some travel and M&S funds. We propose to increase our post-doc support to 100% of 1.0 FTE (two half-time commitments) over the next three years. We envision that one post-doc (likely Onoprienko) will focus on continued algorithm development and the other on user functionality. We also anticipate increased faculty participation by Bolton, Horton-Smith, and Maravin. Travel funds and modest computing support are also requested.

¹⁰ The calorimeter assisted tracking R&D program is carried out at Kansas State University by T.Bolton, G. Horton-Smith, Y. Maravin, D. Onoprienko and E. von Toerne.

¹¹ Not to be confused with the old drift chamber electric field calculation program of the same name.

9.4 Tracking Pattern Recognition Performance

In 2005, the UC Santa Cruz SCIPP group explored the capabilities of the VXDBasedReco algorithm to reconstruct tracks in the SiD detector. A sample of q-qbar events at $E_{\text{cms}}=500$ GeV, with no machine backgrounds, was generated, and the reconstruction efficiency for tracks in the central detector was explored as a function of the angle α between the event thrust axis and the candidate track. The results of this study are shown in Figure 13: the efficiency is independent of the angle α , but only about 94% of the tracks are found.

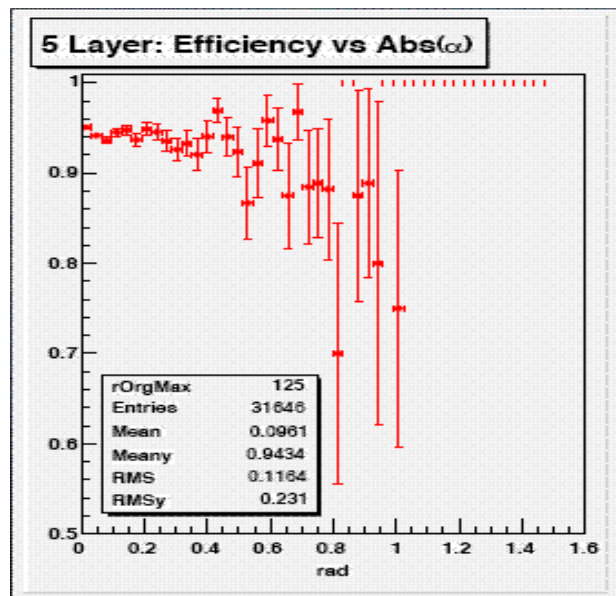


Figure 13: SiD/VXDBasedReco track reconstruction efficiency as a function of angle from the jet core, for q-qbar events at $E_{\text{cms}}=500$ GeV

In fact, VXDBasedReco requires vertex detector segments to seed tracks for the reconstruction, and so it is unable to reconstruct tracks that originate beyond the second layer of the vertex detector. Figure 14 shows the efficiency vs. α strictly for tracks that originate within 1 cm (radially) of the origin. Again, the efficiency is independent of α , but for this sample of prompt tracks, the average efficiency is 99%.

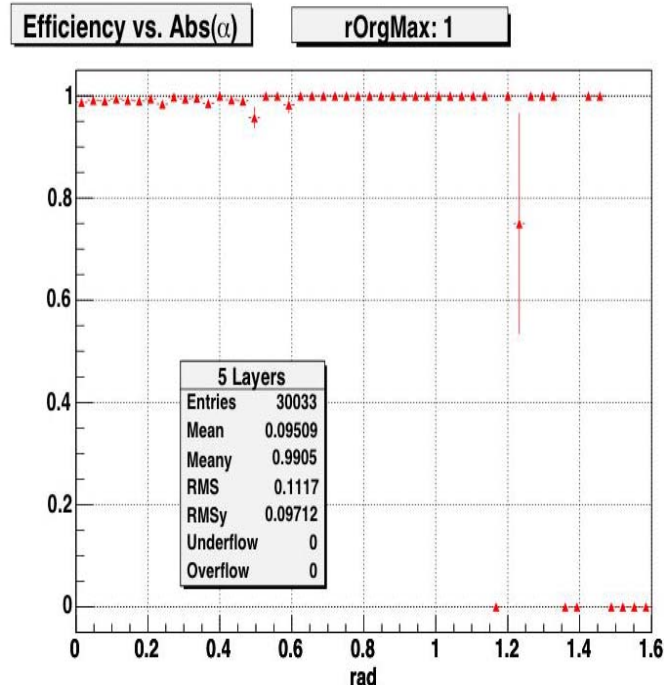


Figure 14: SiD/VXDBasedReco track reconstruction efficiency as a function of angle from the jet core, for $q\text{-}\bar{q}$ events at $E_{\text{cms}}=500$ GeV for prompt tracks (tracks originating within 1cm of the origin).

More recently, SCIPP has adapted the stand-alone reconstruction algorithm described in Section 9.3.3 (AxialBarrelTracker), to find non-prompt tracks among the hits remaining after the reconstruction of prompt tracks. The SCIPP studies began with a characterization of the central tracker hits remaining after the elimination of hits due to prompt tracks.

Hits were assigned to one of four categories: “good”, “looper”, “knock-on”, and “other”, based on the characteristics of the track from which they were associated. “Good” hits are those from tracks with a total momentum is greater than or equal to 1GeV. “Looper” hits are those from tracks with total momentum greater than 10MeV but less than 1GeV, and greater than six hits. “Knock-on” hits are from tracks with total momentum less than or equal to 10MeV, regardless of the number of hits. “Other” hits are from tracks with the same total momentum as looper tracks, but with six or fewer hits per track. The following tables show the breakdown of tracks and hits within these categories. About 6% of remaining hits come from tracks with sufficient momentum that make a single pass through the detector, while almost half (44%) of hits come from non-prompt looping tracks. An additional third (36%) come from very low momentum tracks that are presumably generated by material interactions.

| | | |
|----------------------|--------------|-------------|
| Total tracks: | 6712 | 100% |
| Good tracks: | 445 | 6.6% |
| Looper tracks: | 459 | 6.8% |
| Knock-on tracks: | 3303 | 49.2% |
| Other tracks: | 2505 | 37.3% |
| Total hits: | 30510 | 100% |
| Good hits: | 1754 | 5.7% |
| Looper hits: | 13546 | 44.4% |
| Knock-on hits: | 10821 | 35.5% |
| Other hits: | 4389 | 14.4% |

It's also of interest to explore the radial origin of the tracks that produce the remaining hits. From Figure 15, we see that the majority of "good" tracks have the profile of physics-generated tracks, while the remaining three categories, including "loopers", are dominated by material interactions.

Of great interest, of course, is the percentage of "good" tracks that can be reconstructed. We have explored the efficiency for reconstructing such tracks in the SiD detector with the adapted version of AxialBarrelTracker. In this study, we have assumed only two z segments in each layer, i.e., that each detector layer is composed of two ladders, each of which runs half the length of the layer.

For this study, we have refined the definition of "good" track somewhat, defining a class of "findable" non-prompt particles with the requirements that 1) the particle be charged, and not originate from a material interaction ("backscatter") in the calorimeter; 2) the particle have a radius of origin between 2 cm and 40 cm of the beamline; 3) that the particle have a transverse momentum of greater than 0.75 GeV/c and a path length in the detector of at least 50cm; and 4) the particle have a polar angle θ within $|\cos(\theta)| < 0.8$. In a modest sample of SiD Z-pole b-bbar events, a total of 378 "findable" non-prompt tracks were identified, with an average frequency of roughly two per event, or about 4% of all tracks.

Reconstructed AxialBarrelTracker tracks, which are required to have at least four hits (but can have no more than five hits), were associated with "findable" particles as follows. The "findable" particle that contributed the most hits to the reconstructed track was identified. If the track had four hits, and at least three of these came from the majority "findable" particle, or if the track had five hits, with at least four coming from the majority particle, the "findable" particle was labeled as "found". Any reconstructed track not labeled in this way as "found" was given the label "fake".

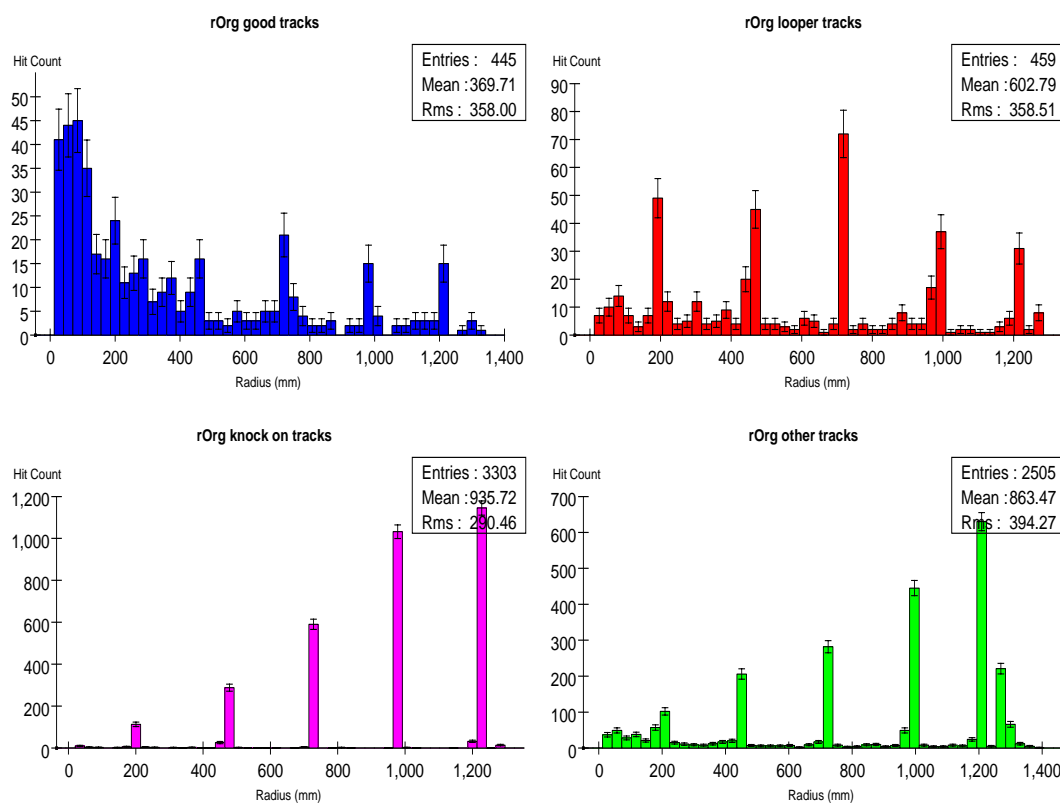


Figure 15: Radial origin of tracks non-prompt tracks. The upper plots, left and right, are for “good” and “looper” tracks, respectively. The lower plots, left and right, are for “knock-on” and “other” tracks, respectively. See the text for a definition of the four categories.

Of the 378 “findable” tracks, a total of 115 (30%) are “found” with five hits, while another 88 (23%) are found with four hits, for a total reconstruction efficiency of 53%. At the same time, though, 327 fake tracks are found, for a total purity of $203/(203+327) = 38\%$. However, all but one of the fake tracks has four hits. Thus, if “found” tracks are required to have exactly five hits, the purity becomes 99%, although the efficiency drops to 30%.

These results are quite preliminary, and there are a number of reasons to expect that they can be significantly improved. Although the SCIPP group adapted AxialBarrelTracker for this second-pass tracking, it has not optimized the routine, and there are a number of ideas that we will explore that we expect will improve the efficiency for finding five-hit tracks. In addition, we will explore the addition of finer (10 cm) z segmentation, as well as the inclusion of additional layers.

The SCIPP group will continue to work, primarily engaging undergraduate thesis students under the direction of Bruce Schumm, to understand the capabilities of the SiD tracking system (including the calorimetry) for reconstructing non-prompt tracks. Current projects include the continued optimization of Tim Nelson’s AxialBarrelTracker as a second-pass algorithm, and the

exploration of the benefit provided to AxialBarrelTracker by the incorporation of the 10cm z segmentation provided by the short-module design. The group will also maintain its basic benchmarking capabilities, and provide feedback to those developing pattern recognition and fitting code for the SiD. Finally, the group hopes to begin to look into the incorporation of calorimeter information in the search for non-prompt tracks, exploring the performance of and then optimizing the Garfield routine provided by the Kansas State group.

By the end of 2007, we hope to have optimized AxialBarrelTracker and explored its dependence upon z segmentation, as well as provided basic benchmarking studies of any new recognition/fitting algorithms that become available. In 2008, we hope to turn to the incorporation and optimization of the Garfield package as a third-pass algorithm for finding non-prompt tracks. We plan to maintain our benchmarking capabilities during this period.

9.5 Tracking Resolution Studies

The tracker momentum resolution can be studied using track fitting software developed by the University of Oregon group. This software is similar to that used in the SLD experiment and is based on the use of a measurements weight matrix that incorporates both measurement errors and the fully correlated multiple scattering errors.

The software is implemented in the framework of Java Analysis Studio, as part of the org.lcsim package. The track fitting algorithm finds 5 track parameters that best fit the measured hit positions in all layers of tracker and vertex detectors. To do this, measurement weights are assigned to each hit position measurement, based on the expected multiple scattering of the track due to material in the path of the charged particle. The sensor spatial resolution is also taken into account. Hit position displacements due to multiple scattering are not independent in subsequent detector layers, and such displacement correlations are taken into account in the weight matrix.

Fitting is achieved by solving minimization equations for a measurement χ^2 expressed as a function of measurements residuals (difference between hit position and calculated position of track intersection with sensor) and weights. The fitting procedure provides not only best fitted values for track parameters, but also an estimation of the errors on these parameters (parameters covariance matrix).

The track fitting algorithm was thoroughly checked to ensure that the error estimations are in good agreement with the deviation between the fitted parameters and the true Monte Carlo values. For this simulation, the generated Geant4 charged track hits were used with Gaussian smearing. Residual distributions of the track parameters normalized to the covariance matrix all had sigma equal to 1, confirming that the correct errors are assigned to the track parameters.

The track parameter covariance matrix does not depend on the measured hit positions, but only on the particle momentum, amount and distribution of materials in the particle path, and sensor accuracy. Thus, the covariance matrix for a given set of track parameters can be calculated without simulating the actual particle propagation. This fitter feature allows investigation of the tracking resolution for different detector configurations without requiring time consuming Geant4 simulations.

The results of these investigations are shown in the figures below. The two top plots in Figure 16 show the tracker momentum resolution as a function of polar angle achieved for the current tracker geometry (SiD01) and an earlier version of the Sid tracker geometry (SiDAug05). The lower two plots in Figure 16 shows the tracker momentum resolution as a function of transverse momentum for tracks at 90° . Excellent momentum resolution is achieved in the SiD detector, with $\sigma(p_T)/p_T < 0.2\%$ for tracks at 90° for track momenta up to 100 GeV. These figures also show the results from a Billoir-based track-parameter error estimation tool¹², which is used for the “fast Monte Carlo” studies. The weight matrix and Billoir-based track fitters are seen to be in good agreement.

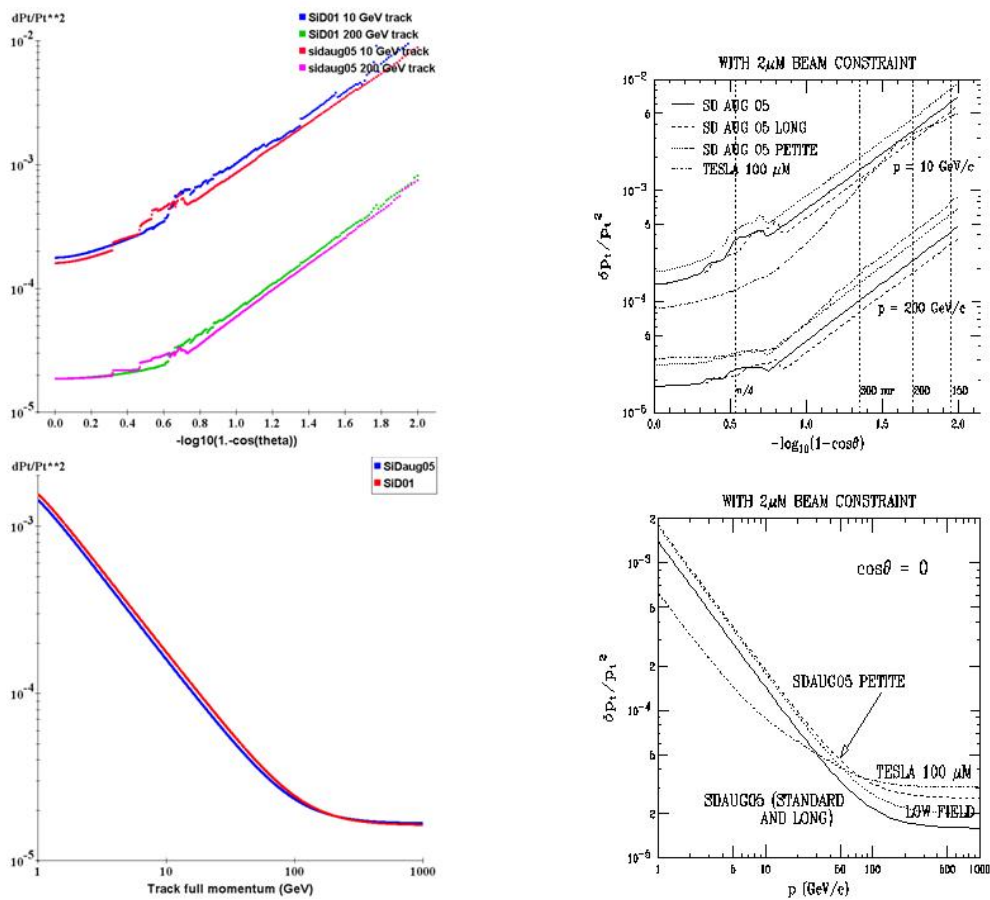


Figure 16: Track momentum resolution vs $\cos\theta$ for weight matrix fitter (top left) and Billoir fitter (top right). Tracker momentum resolution vs track momentum for the weight matrix fitter (lower left) and Billoir fitter (lower right)

¹² B. A. Schumm, <http://www.slac.stanford.edu/~schumm/lcdtrk20011204.tar.gz>

9.6 R&D Plans for Tracking Simulation and Performance Studies

Substantial effort has been put into developing the simulation infrastructure, track finding algorithms, and track fitting algorithms. While preliminary results are encouraging, there remains substantial R&D needed in the area of tracker simulation. The coming months will see a repeated cycle of upgrading the detail and fidelity of the simulation, upgrading the reconstruction code and upgrading the simulated analyses. At the completion of each cycle, the sensitivity of the detector for the relevant benchmark physics processes will be evaluated. Some of the studies that are foreseen include:

1. Improve the level of detail in the model of the forward tracking system, including the study of various sensor geometries and strip orientation.
2. Study variations in the baseline design to optimize the tracker design. Among the parameters that we plan to study are the number of tracker layers, the size of the tracking volume, the location of tracker layers within the tracking volume, and the effect of incorporating stereo layers and/or charge division readout in the design.
3. Evaluate the robustness of the pattern recognition algorithms against the levels of various backgrounds including, machine backgrounds from lost upstream particles, e^+e^- pairs, and back-scattered photons, two photon interactions, knock-on particles, and electronic noise. For candidate technologies that integrate over multiple bunch crossings it will be important to correctly model the additional confusion.
4. Evaluate the impact of dead material in the tracker on the particle flow algorithms and the resulting effect on physics sensitivity, and study the effect of changing the amount and location of dead material.
5. Understand which detector properties are limiting physics performance: resolution, material budget, closeness to the IP, and so on.
6. Continue the development of algorithms for the classification of jets as b-quark, c-quark or light quarks and work and iterate, in collaboration with the vertex detector group, on the optimization of the tracker for flavor identification.

10 SUMMARY OF R&D NEEDS

The tables below summarize the R&D needs over the next few years for all the universities and laboratories involved in the SiD tracker. M&S numbers are in kilo-dollars and manpower estimates are in FTE's.

| Kansas State University | FY05 | | FY06 | | FY07 | | FY08 | | FY09 | | FY10 | | FY11 | | Total Cost |
|-------------------------|------|-----------|------|-----------|------|-----------|------|-----------|------|-----------|------|-----------|------|-----------|------------|
| | Need | Cost(K\$) | |
| M&S | | \$ - | | \$ - | 7 | \$ 7 | 17 | \$ 17 | 20 | \$ 20 | 20 | \$ 20 | | \$ - | \$ 64 |
| Postdocs | | \$ - | | \$ - | 0.2 | \$ 18 | 1 | \$ 90 | 1 | \$ 90 | 1 | \$ 90 | | \$ - | \$ 288 |
| TOTAL | | \$ - | | \$ - | | \$ 25 | | \$ 107 | | \$ 110 | | \$ 110 | | \$ - | \$ 352 |

Table 10: Kansas State University R&D effort for development of calorimeter assisted tracking.

| U of Mich | FY05 | | FY06 | | FY07 | | FY08 | | FY09 | | FY10 | | FY11 | | Total Cost |
|--------------|------|-----------|------|-----------|------|-----------|------|-----------|------|-----------|------|-----------|------|-----------|------------|
| | Need | Cost(K\$) | |
| M&S | | \$ - | | \$ - | 3 | \$ 3 | 6 | \$ 6 | 10 | \$ 10 | 10 | \$ 10 | 6 | \$ 6 | \$ 35 |
| Postdocs | | \$ - | | \$ - | 0.7 | \$ 63 | 0.7 | \$ 63 | 0.7 | \$ 63 | 0.7 | \$ 63 | 0.7 | \$ 63 | \$ 315 |
| Staff | | \$ - | | \$ - | 0 | \$ - | | \$ - | | \$ - | | \$ - | | \$ - | \$ - |
| EE | | \$ - | | \$ - | 0 | \$ - | | \$ - | | \$ - | | \$ - | | \$ - | \$ - |
| ME | | \$ - | | \$ - | 0 | \$ - | | \$ - | | \$ - | | \$ - | | \$ - | \$ - |
| students | | \$ - | | \$ - | 0.5 | \$ 30 | 0.5 | \$ 30 | 0.5 | \$ 30 | 0.5 | \$ 30 | 0.5 | \$ 30 | \$ 150 |
| techs | | \$ - | | \$ - | 0 | \$ - | 0.25 | \$ 17 | 0.25 | \$ 17 | 0.25 | \$ 17 | 0.25 | \$ 17 | \$ 68 |
| TOTAL | | \$ - | | \$ - | | \$ 96 | | \$ 116 | | \$ 120 | | \$ 120 | | \$ 116 | \$ 568 |

Table 11: University of Michigan R&D effort for development of the alignment system and benchmarking studies

| Software | Brown | FY05 | | FY06 | | FY07 | | FY08 | | FY09 | | FY10 | | FY11 | | Total Cost |
|----------|--------------|------|-----------|------|-----------|------|-----------|------|-----------|------|-----------|------|-----------|------|-----------|------------|
| | | Need | Cost(K\$) | |
| Software | M&S | | \$ - | | \$ - | 25 | \$ 25 | 25 | \$ 25 | 75 | \$ 75 | | \$ - | | \$ - | \$ 125 |
| Software | Postdocs | 0.2 | \$ 18 | | \$ - | | \$ - | | \$ - | | \$ - | | \$ - | | \$ - | \$ 18 |
| Software | TOTAL | | \$ 18 | | \$ - | | \$ 25 | | \$ 25 | | \$ 75 | | \$ - | | \$ - | \$ 143 |

Table 12: Brown University R&D effort for development of tracking software and charge division readout.

| Purdue | FY05 | | FY06 | | FY07 | | FY08 | | FY09 | | FY10 | | FY11 | | Total Cost |
|--------------|------|-----------|------|-----------|------|-----------|------|-----------|------|-----------|------|-----------|------|-----------|------------|
| | Need | Cost(K\$) | |
| M&S | | \$ - | | \$ - | 9 | \$ 9 | 4 | \$ 4 | 5 | \$ 5 | 5 | \$ 5 | 5 | \$ 5 | \$ 28 |
| Postdocs | | \$ - | | \$ - | 0 | \$ - | 0.5 | \$ 45 | 0.5 | \$ 45 | 1 | \$ 90 | 1 | \$ 90 | \$ 270 |
| Staff | | \$ - | | \$ - | 0 | \$ - | 0 | \$ - | 0 | \$ - | 0 | \$ - | 0 | \$ - | \$ - |
| EE | | \$ - | | \$ - | 0.2 | \$ 24 | 0.2 | \$ 24 | 0.2 | \$ 24 | 0.2 | \$ 24 | 0.25 | \$ 31 | \$ 128 |
| ME | | \$ - | | \$ - | 0.2 | \$ 24 | 0.2 | \$ 24 | 0.2 | \$ 24 | 0.2 | \$ 24 | 0.25 | \$ 31 | \$ 128 |
| students | | \$ - | | \$ - | 0.5 | \$ 30 | 0.5 | \$ 30 | 0.5 | \$ 30 | 1 | \$ 60 | 1 | \$ 60 | \$ 210 |
| techs | | \$ - | | \$ - | 0.2 | \$ 14 | 0.2 | \$ 14 | 0.2 | \$ 14 | 0.2 | \$ 14 | 0.25 | \$ 17 | \$ 71 |
| TOTAL | | \$ - | | \$ - | | \$ 101 | | \$ 141 | | \$ 142 | | \$ 217 | | \$ 233 | \$ 836 |

Table 13: Purdue University R&D effort on thin silicon. .

SID Tracker R&D

| Colorado | FY05 | FY05 | FY06 | FY06 | FY07 | FY07 | FY08 | FY08 | FY09 | FY09 | FY10 | FY10 | FY11 | FY11 | Total |
|--------------|-------|-----------|-------|-----------|------|-----------|------|-----------|------|-----------|------|-----------|------|-----------|--------|
| | Need | Cost(K\$) | Need | Cost(K\$) | Need | Cost(K\$) | Need | Cost(K\$) | Need | Cost(K\$) | Need | Cost(K\$) | Need | Cost(K\$) | |
| M&S | 3 | \$ 3 | 6 | \$ 6 | 5 | \$ 5 | 5 | \$ 5 | 5 | \$ 5 | 5 | \$ 5 | 5 | \$ 5 | \$ 34 |
| Postdocs | 0.26 | \$ 23 | 0.277 | \$ 25 | | \$ - | | \$ - | | \$ - | | \$ - | | \$ - | \$ 48 |
| Staff | | \$ - | | \$ - | 0.2 | \$ 26 | 0.2 | \$ 26 | 0.2 | \$ 26 | 0.2 | \$ 26 | 0.2 | \$ 26 | \$ 128 |
| EE | | \$ - | | \$ - | | \$ - | | \$ - | | \$ - | | \$ - | | \$ - | \$ - |
| ME | | \$ - | | \$ - | | \$ - | | \$ - | | \$ - | | \$ - | | \$ - | \$ - |
| students | 0.017 | \$ 1 | | \$ - | | \$ - | | \$ - | | \$ - | | \$ - | | \$ - | \$ 1 |
| TOTAL | | \$ 27 | | \$ 31 | | \$ 31 | | \$ 31 | | \$ 31 | | \$ 31 | | \$ 31 | \$ 211 |

Table 14: University of Colorado R&D effort on tracking software development..

| Oregon | FY05 | FY05 | FY06 | FY06 | FY07 | FY07 | FY08 | FY08 | FY09 | FY09 | FY10 | FY10 | FY11 | FY11 | Total |
|--------------|------|-----------|------|-----------|------|-----------|------|-----------|------|-----------|------|-----------|------|-----------|--------|
| | Need | Cost(K\$) | |
| M&S | 5 | \$ 5 | 5 | \$ 5 | 5 | \$ 5 | 5 | \$ 5 | 5 | \$ 5 | 5 | \$ 5 | | \$ - | \$ 30 |
| Postdocs | | \$ - | | \$ - | | \$ - | | \$ - | | \$ - | | \$ - | | \$ - | \$ - |
| Staff | 0.25 | \$ 32 | 0.25 | \$ 32 | 0.25 | \$ 32 | 0.25 | \$ 32 | 0.25 | \$ 32 | 0.25 | \$ 32 | | \$ - | \$ 192 |
| TOTAL | | \$ 37 | | \$ 37 | | \$ 37 | | \$ 37 | | \$ 37 | | \$ 37 | | \$ - | \$ 222 |

Table 15: University of Oregon R&D effort on development of tracking software.

| Santa Cruz | FY05 | FY05 | FY06 | FY06 | FY07 | FY07 | FY08 | FY08 | FY09 | FY09 | FY10 | FY10 | FY11 | FY11 | Total |
|--------------|------|-----------|------|-----------|------|-----------|------|-----------|------|-----------|------|-----------|------|-----------|---------|
| | Need | Cost(K\$) | |
| M&S | 0 | \$ - | 0 | \$ - | 45 | \$ 45 | 45 | \$ 45 | 45 | \$ 45 | 20 | \$ 20 | 20 | \$ 20 | \$ 175 |
| Postdocs | 0 | \$ - | 0 | \$ - | 0.5 | \$ 45 | 0.5 | \$ 45 | 0.5 | \$ 45 | 0 | \$ - | 0 | \$ - | \$ 135 |
| Staff | 0 | \$ - | 0 | \$ - | 0.5 | \$ 64 | 0.5 | \$ 64 | 0.5 | \$ 64 | 0 | \$ - | 0 | \$ - | \$ 192 |
| EE | 0 | \$ - | 0 | \$ - | 1.2 | \$ 146 | 1.2 | \$ 146 | 1.2 | \$ 146 | 0 | \$ - | 0 | \$ - | \$ 439 |
| ME | 0 | \$ - | 0 | \$ - | 0 | \$ - | 0 | \$ - | 0 | \$ - | 0 | \$ - | 0 | \$ - | \$ - |
| students | 0 | \$ - | 0.3 | \$ 18 | 0.8 | \$ 48 | 0.8 | \$ 48 | 0.8 | \$ 48 | 0.3 | \$ 18 | 0.3 | \$ 18 | \$ 198 |
| techs | 0 | \$ - | 0 | \$ - | 0.5 | \$ 34 | 0.5 | \$ 34 | 0.5 | \$ 34 | 0 | \$ - | 0 | \$ - | \$ 102 |
| TOTAL | | \$ - | | \$ 18 | | \$ 382 | | \$ 382 | | \$ 382 | | \$ 38 | | \$ 38 | \$1,241 |

Table 16: University of California at Santa Cruz R&D effort on benchmarking studies, time-over-threshold readout and charge division readout.

| New Mexico | FY05 | FY05 | FY06 | FY06 | FY07 | FY07 | FY08 | FY08 | FY09 | FY09 | FY10 | FY10 | FY11 | FY11 | Total |
|--------------|------|-----------|------|-----------|------|-----------|------|-----------|------|-----------|------|-----------|------|-----------|--------|
| | Need | Cost(K\$) | |
| M&S | 0 | \$ - | 0 | \$ - | 50 | \$ 50 | 10 | \$ 10 | 50 | \$ 50 | 10 | \$ 10 | 0 | \$ - | \$ 120 |
| Postdocs | 0 | \$ - | 0 | \$ - | 0.5 | \$ 45 | 0.5 | \$ 45 | 0.5 | \$ 45 | 0 | \$ - | 0 | \$ - | \$ 135 |
| Staff | 0 | \$ - | 0 | \$ - | 0.25 | \$ 32 | 0 | \$ - | 0.25 | \$ 32 | 0 | \$ - | 0 | \$ - | \$ 64 |
| EE | 0 | \$ - | 0 | \$ - | 0.6 | \$ 73 | 0.6 | \$ 73 | 0.35 | \$ 43 | 0.25 | \$ 31 | 0 | \$ - | \$ 220 |
| ME | 0 | \$ - | 0 | \$ - | 0 | \$ - | 0 | \$ - | 0 | \$ - | 0 | \$ - | 0 | \$ - | \$ - |
| students | 0 | \$ - | 0 | \$ - | 0.95 | \$ 57 | 0.7 | \$ 42 | 0.95 | \$ 57 | 0.25 | \$ 15 | 0 | \$ - | \$ 171 |
| techs | 0 | \$ - | 0 | \$ - | 0 | \$ - | 0 | \$ - | 0 | \$ - | 0 | \$ - | 0 | \$ - | \$ - |
| TOTAL | | \$ - | | \$ - | | \$ 257 | | \$ 170 | | \$ 227 | | \$ 56 | | \$ - | \$ 710 |

Table 17: University of New Mexico R&D effort on sensor testing and the design of the sensor module readout cable.

| SLAC | FY05 | | FY06 | | FY07 | | FY08 | | FY09 | | FY10 | | FY11 | | Total Cost |
|--------------|------|-----------|------|-----------|-------|-----------|-------|-----------|-------|-----------|-------|-----------|-------|-----------|---------------|
| | Need | Cost(K\$) | Need | Cost(K\$) | Need | Cost(K\$) | Need | Cost(K\$) | Need | Cost(K\$) | Need | Cost(K\$) | Need | Cost(K\$) | |
| M&S | | \$ - | | \$ - | 150.5 | \$ 151 | 147.5 | \$ 148 | 130 | \$ 130 | 132.5 | \$ 133 | 0 | \$ - | \$ 561 |
| Postdocs | | \$ - | | \$ - | 0 | \$ - | 0.25 | \$ 23 | 0.25 | \$ 23 | 0.25 | \$ 23 | 0.375 | \$ 34 | \$ 101 |
| Staff | | \$ - | | \$ - | 1.75 | \$ 224 | 1.75 | \$ 224 | 0.625 | \$ 80 | 0.375 | \$ 48 | 0.25 | \$ 32 | \$ 608 |
| EE | | \$ - | | \$ - | 0.5 | \$ 61 | 0.5 | \$ 61 | 0 | \$ - | 0 | \$ - | 0 | \$ - | \$ 122 |
| ME | | \$ - | | \$ - | 0.25 | \$ 31 | 0.625 | \$ 76 | 0.5 | \$ 61 | 0.25 | \$ 31 | 0 | \$ - | \$ 198 |
| students | | \$ - | | \$ - | 0.25 | \$ 15 | 1.5 | \$ 90 | 1.75 | \$ 105 | 0.75 | \$ 45 | 0.5 | \$ 30 | \$ 285 |
| techs | | \$ - | | \$ - | 0.625 | \$ 43 | 0.5 | \$ 34 | 1 | \$ 68 | 0.375 | \$ 26 | 0.125 | \$ 9 | \$ 179 |
| TOTAL | | \$ - | | \$ - | | \$ 524 | | \$ 655 | | \$ 467 | | \$ 304 | | \$ 104 | \$2,054 |

Table 18: SLAC R&D effort on sensor and module design, mechanical design, software development, development of the readout chip and readout cable and power distribution and DAQ.

| Fermilab | FY05 | | FY06 | | FY07 | | FY08 | | FY09 | | FY10 | | FY11 | | Total Cost |
|--------------|------|-----------|------|-----------|-------|-----------|-------|-----------|-------|-----------|-------|-----------|-------|-----------|---------------|
| | Need | Cost(K\$) | Need | Cost(K\$) | Need | Cost(K\$) | Need | Cost(K\$) | Need | Cost(K\$) | Need | Cost(K\$) | Need | Cost(K\$) | |
| M&S | | \$ - | | \$ - | 86.5 | \$ 87 | 153.5 | \$ 154 | 880 | \$ 880 | 518.5 | \$ 519 | 10 | \$ 10 | \$1,649 |
| Postdocs | | \$ - | | \$ - | 0 | \$ - | 0.25 | \$ 23 | 0.25 | \$ 23 | 0.25 | \$ 23 | 0.375 | \$ 34 | \$ 101 |
| Staff | | \$ - | | \$ - | 2.925 | \$ 374 | 3.275 | \$ 419 | 3.15 | \$ 403 | 1.075 | \$ 138 | 0.7 | \$ 90 | \$1,424 |
| EE | | \$ - | | \$ - | 0 | \$ - | 0 | \$ - | 0 | \$ - | 0 | \$ - | 0 | \$ - | \$ - |
| ME | | \$ - | | \$ - | 2.26 | \$ 276 | 3.69 | \$ 450 | 2.425 | \$ 296 | 1.85 | \$ 226 | 1.35 | \$ 165 | \$1,412 |
| students | | \$ - | | \$ - | 0.25 | \$ 15 | 1.5 | \$ 90 | 1.25 | \$ 75 | 0.75 | \$ 45 | 0.5 | \$ 30 | \$ 255 |
| techs | | \$ - | | \$ - | 0.735 | \$ 50 | 1.515 | \$ 103 | 2.875 | \$ 196 | 3.175 | \$ 216 | 2.825 | \$ 192 | \$ 757 |
| TOTAL | | \$ - | | \$ - | | \$ 802 | | \$1,238 | | \$1,872 | | \$1,165 | | \$ 520 | \$5,597 |

Table 19: Fermilab R&D effort on sensor and module design, mechanical design and software development.

11 SUMMARY

The characteristics of the ILC pose many new challenges for the detector community. One of the characteristics of the e^+e^- collider is that most processes occur with electroweak couplings and have rather small cross sections. The intense beams on the other hand, give rise to high backgrounds in the vertex and forward detectors. In contrast to previous experiments at e^+e^- colliders, where most events of interest are produced in the central region, at the ILC there are in addition fundamental processes in the forward region. In fact, many physics processes with polarized beams show the greatest sensitivity to deviations from the standard model for events in the forward regions.

If new physics exists at lower energies it may well be uncovered by the LHC. One critical role for the ILC will thus be to carry out precision measurements relevant to newly discovered physics and determine unambiguously the parameters which characterize it. In this role, great importance is placed on precision. This in turn has significant implications for the detector design.

It is fair to say that in many existing collider experiments the forward tracking detectors were far from optimal. Given the low event rates at the ILC, the mixed success of the physics community in designing and building low mass vertex detectors and trackers optimized for the forward regions, significant R&D is needed not just in the mechanical design but also in the area of simulation to ensure high tracking efficiency and excellent heavy flavor identification. The SiD tracker must reconstruct charged tracks with high efficiency, measure track parameters with excellent precision, and minimize the impact of multiple scattering and secondary interactions caused by the tracker material over the full angular coverage. Hence the R&D program outlined in this report. The SiD tracker puts a premium on compact, low mass, integrated tracking. It is envisioned that this is accomplished with large diameter, nested, carbon-fiber support structures. The basic building block of the tracker is a silicon module with dual bump-bonded front-end ASIC, with readout and power through a single flexible cable. Basic R&D needs to be carried out to verify the viability of this concept.

Alternative approaches, including thin silicon sensors, charge division and time-over-threshold will also be investigated. A significant amount of work still needs to be carried out to benchmark the physics performance of the proposed vertex detector and outer tracker. The software developed to date is not yet in a position to answer the physics reach and physics compromises of the current design at a satisfactory level. Tracking simulation and reconstruction thus needs further development as well.